Barium β-Ketoiminate Complexes Containing Appended Ether "Lariats". Synthesis, Characterization, and Implementation as Fluorine-Free Barium MOCVD Precursors

Douglas L. Schulz,† Bruce J. Hinds, Deborah A. Neumayer, Charlotte L. Stern, and Tobin J. Marks*

Department of Chemistry, the Materials Research Center, and the Science and Technology Center for Superconductivity, Northwestern University, Evanston, Illinois 60208-3113

Received March 19, 1993. Revised Manuscript Received August 9, 1993®

The synthesis and characterization of six volatile fluorine-free barium coordination complexes based upon encapsulating β-ketoiminate ether/polyether ligation and having the general formula $Ba(RCOCHC(NR')R'')_2$ (R = *tert*-butyl; R' = $CH_2CH_2OCH_3$, $-(CH_2CH_2O-)_2CH_3$, $-(CH_2CH_2O-)_3CH_2CH_3$; and R'' = methyl or *tert*-butyl) is reported. The complexes were prepared by a nonaqueous approach which employs BaH_2 and the corresponding β-ketoimine. These complexes have been characterized by ^1H and ^{13}C NMR spectroscopy, elemental analysis, mass spectroscopy, cryoscopy, and thermogravimetric analysis. Single-crystal X-ray structural analysis of bis[2,2-dimethyl-5-*N*-(2-(2-methoxy)ethoxyethylimino)-3-hexanonato]barium(II) reveals a monomeric eight-coordinate, distorted dodecahedral configuration about barium: space group = $C2/c$; a = 32.764(6) Å, b = 12.110(2) Å, c = 15.690(5) Å, β = 102.12(2), Z = 8; $R(F)$ = 0.044, $R_W(F)$ = 0.040 for 2776 reflections having $I > 3\sigma(I)$. Single-crystal X-ray structural analysis of bis[2,2-dimethyl-5-*N*-(2-(2-(2-ethoxy)ethoxy)ethoxyethylimino)-3-hexanonato]barium(II) also reveals a monomeric eight-coordinate distorted dodecahedral configuration about barium: space group = $Pccn$; a = 24.939(4) Å, b = 10.546(2) Å, c = 14.349(4) Å, Z = 4; $R(F)$ = 0.036; $R_W(F)$ = 0.035 for 1689 reflections having $I > 3\sigma(I)$. Single-crystal X-ray structural analysis of bis[5-*N*-(2-methoxyethylimino)-2,2,6,6-tetramethyl-3-heptanonato]barium(II) indicates a nearly symmetric $Ba_2(\mu_2$-*O*-ketoiminate$)_2$ dimeric structure. Each half of the dimer possesses a distorted pentagonal pyramidal local configuration about the barium ion with an unusual O, O coordination of one of the ketoiminate rings: space group = $C2/c$; a = 27.687(5) Å, b = 10.453(2) Å, c = 22.679(6) Å, β = 101.88(2), Z = 8; $R(F)$ = 0.033, $R_W(F)$ = 0.042 for 4881 reflections having $I > 3\sigma(I)$. These complexes are volatile and can be used as MOCVD precursors. Thus, $BaPbO_3$ films have been grown using these complexes and Pb(dipivaloylmethanate)$_2$ and have been characterized by X-ray diffraction, scanning electron microscopy energy-dispersive X-ray spectroscopy, and variable-temperature resistivity measurements. Thermolytic decomposition of the barium β-ketoiminate complexes involves cleavage of the C–O bond β to nitrogen and affords pinacolone, 2,2-dimethyl-5-imino-3-hexanone, and 2-methyl-4-*tert*-butylpyridine as the major organic thermolysis products.

Introduction

Minimizing molecular oligomerization, and hence lattice cohesive energies, by saturating the metal coordination sphere with sterically encumbered nonpolar or fluorinated ligands is an attractive strategy for the design of volatile MOCVD (metal–organic chemical vapor deposition) precursors. Monomeric complexes are expected to exhibit enhanced volatility in comparison to oligomeric complexes in which intermolecular solid-state interactions/connectivities are likely to increase the enthalpy of vaporization. In addition to favorable and stable vapor pressure characteristics, a useful MOCVD precursor must also have appropriate reactivity for the desired film growth process. Chemical flexibility, whereby ligand modifications effect tunability of these parameters, is also desirable.

For the MOCVD growth of barium-containing ferroelectric[1] or high-T_c superconducting films,[2-4] the small charge-to-radius ratio of Ba^{2+} presents a significant

† Present address: National Renewable Energy Laboratory, Golden, CO 80401-3393.

® Abstract published in *Advance ACS Abstracts*, October 1, 1993.

(1) (a) Lu, H. A.; Wills, L. A.; Wessels, B. W.; Lin, W. P.; Zhang, T. J.; Wong, G. K.; Neumayer, D. A.; Marks, T. J. *Appl. Phys. Lett.* **1993**, *62*, 1314. (b) Wills, L. A.; Wessels, B. W.; Richeson, D. S.; Marks, T. J. *Appl. Phys. Lett.* **1992**, *60*, 41. (c) Van Buskirk, P. C.; Gardiner, R.; Kirlin, P. S.; Nutt, S. *J. Mater. Res.* **1992**, *7*, 542.

(2) (a) Malandrino, G.; Richeson, D. S.; Marks, T. J.; DeGroot, D. C.; Kannewurf, C. R. *Appl. Phys. Lett.* **1991**, *58*, 182. (b) Zhang, J. M.; Wessels, B. W.; Richeson, D. S.; Marks, T. J.; DeGroot, D. C.; Kannewurf, C. R. *J. Appl. Phys.* **1991**, *69*, 2743. (c) Duray, S. J.; Buchholz, D. B.; Song, S. N.; Richeson, D. S.; Ketterson, J. B.; Marks, T. J.; Chang, R. P. H. *Appl. Phys. Lett.* **1991**, *59*, 1503. (d) Zhang, J.; Zhao, J.; Marcy, H. O.; Tonge, L. M.; Wessels, B. W.; Marks, T. J.; Kannewurf, C. R. *Appl. Phys. Lett.* **1989**, *54*, 1166. (e) Richeson, D. S.; Tonge, L. M.; Zhao, J.; Zhang, J.; Marcy, H. O.; Marks, T. J.; Wessels, B. W.; Kanneworf, C. R. *Appl. Phys. Lett.* **1989**, *54*, 2154.

(3) (a) Zhang, K.; Erbil, A. *Mater. Sci. Forum*, in press, and references therein. (b) Hirai, T.; Yamane, H. *J. Cryst. Growth* **1991**, *107*, 683.

(4) (a) Zhao, J.; Li, Y. Q.; Chern, C. S.; Lu, P.; Norris, P.; Gallois, B.; Kear, B.; Cosandey, F.; Wu, X. D.; Muenchausen, R. E.; Garrison, S. M. *Appl. Phys. Lett.* **1991**, *59*, 1254. (b) Spee, C. I. M. A.; Vander Zouwen-Assink, E. A.; Timmer, K.; Mackor, A.; Meinema, H. A. *J. Phys. IV* **1991**, *1*, C2/295.

0897-4756/93/2805-1605$04.00/0

challenge in precursor ligand design.[5] Nonfluorinated β-diketonate precursors such as "Ba(dpm)$_2$" (dpm = dipivaloylmethanate) suffer from compositional uncertainties[6] as well as a less than optimum, variable, and unstable vapor pressure.[6a,7] Coordinatively saturated fluorinated β-diketonate precursors such as Ba(hfa)$_2$·tetraglyme (hfa = hexafluoroacetylacetonate)[5c] represent a significant advance in vapor pressure characteristics; however, deposition processes usually require an additional H_2O/O_2 annealing treatment to eliminate contaminating fluoride phases from the resultant films.[2a-c,4b] These limitations associated with known barium MOCVD precursors illustrate the potential attraction of nonfluorinated, coordinatively saturated, volatile barium complexes of well-defined and reproducible stoichiometry.

β-Ketoiminates offer a potential means to address the aforementioned issues since N-derivatization offers an appendage point for additional intramolecular coordination/saturation of Ba^{2+} ion. The synthesis, characterization, and eventual implementation of such ligands containing appended ether "lariats" (e.g., I) was the primary

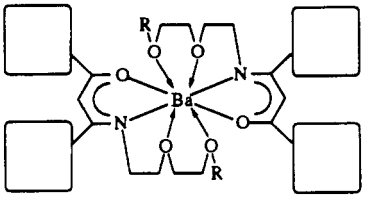

I

goal of this study. The tendency of an ether-functionalized β-ketoiminate imine to coordinate in an intramolecular fashion has already been established in the case of six-coordinate bis[(*N*-alkoxyalkyl)salicylaldimine]nickel(II) complexes.[8] Furthermore, suitable gas-phase reactivity of simple β-ketoiminate complexes in MOCVD processes has been demonstrated by the growth of $YBa_2Cu_3O_7$ thin films using bis(4-imino-2-pentanato)copper(II) as the volatile copper precursor.[9] Beyond providing potentially monomeric, volatile precursor complexes, β-ketoiminates may also fulfull other requirements of useful barium MOCVD precursors. Thus, the ability to functionalize the imino residue of the β-ketoimine ligand with different types and lengths of lariats offer potential tailoring of thermal characteristics (e.g., volatility and melting point) in the resulting barium complexes—a capacity not realizable with many other ligand systems.

We report here the synthesis and structural characterization of six fluorine-free and, in some cases, monomeric barium MOCVD precursors based upon encapsulating β-ketoiminate ether/polyether ligands (I). A comparison of the physical properties of these complexes is made with the common barium MOCVD precursor "Ba(dpm)$_2$". A volatile barium β-ketoiminate complex is then used in combination with Pb(dpm)$_2$ as precursors for the MOCVD growth of $BaPbO_3$ (a metallike pervoskite[10]) films. The thermolytic behavior of the barium β-ketoiminate complexes, which sublime with partial decomposition, is also investigated, and evidence for a unique thermolysis mechanism presented.

Experimental Section

General Procedures. Standard Schlenk techniques and a Vacuum Atmospheres nitrogen-filled glovebox were used in the isolation and handling of β-ketoimines and barium β-ketoiminate complexes. Diethyl ether and THF solvents were dried over Na ribbon prior to use. Pentane and heptane were dried over sodium benzophenone ketyl and distilled immediately prior to use. Pyridine was dried over NaOH pellets prior to use. ^1H and ^{13}C NMR spectra were recorded in CD_3OD, $CDCl_3$, or dry, deoxygenated C_6D_6, toluene-d_8, or THF-d_8 on either a Varian Gemini 300 or a Varian XLA 400 spectrometer. Chemical shifts for ^1H and ^{13}C spectra were referenced to solvent signals. Electron impact mass spectra were obtained on a VG 70-250 SE spectrometer using an ionization potential of 70 eV with a temperature ramping rate of 20 °C/s from ambient to 200 °C. Liquids and solids loaded in capillary tubes were introduced via a direct insertion probe. Gas chromatography/electron impact mass spectra were obtained using a Hewlett-Packard 5890 GC interfaced to a VG-70-250 SE spectrometer. A 15-m narrow-bore J&W Scientific DB-1 fused silica capillary with 1.0-μm film thickness was employed as the column material. An ion source potential of 70 eV, an inlet source temperature of 200 °C, and a column temperature ramp rate of 20 °C/min from ambient to 200 °C were used in GC/MS experiments. All mass spectra were calibrated using PCR perfluorokerosene 755. Cryoscopic molecular weights under inert atmosphere were determined with a modified Knauer 24.00 cryoscopic unit using benzene, vacuum transferred from Na–K alloy, as the solvent. A bibenzyl solution was used as a calibration standard, with a solvent reference and standard reference scan performed after every unknown determination. Thermogravimetric analyses were performed under an N_2 atmosphere on a Perkin-Elmer TGA7 thermogravimetric analyzer with a temperature ramp of 10 °C/min from 50 to 500 °C. Elemental analyses were performed by either G.D. Searle, Inc. (Skokie, IL) or Galbraith Laboratories, Inc. (Knoxville, TN).

Glassware used in synthesis and reaction of silyl enol ether derivatives was subjected to the following treatment: (1) 1-h rinse in KOH/isopropyl alcohol; (2) distilled water rinse followed by a 20-min oven dry; (3) the surface was silated by addition of hexamethyldisilane and a heat gun thermal treatment with the remaining residue being removed in vacuo.

Reagents. The β-diketone 2,2-dimethyl-3,5-hexanedione was prepared according to the literature procedure,[11] while 2,2,6,6-tetramethyl-3,5-heptanedione (Hdpm) was obtained from Lancaster Synthesis, BaH_2 (95% metals purity) from Strem, methyl iodide from Mallinckrodt, and 2-ethoxyethanol, 2-(2-aminoethoxy)ethanol, and *p*-toluenesulfonyl chloride from Aldrich. All of these reagents were used as received. The reagent 2-methoxyethylamine was purchased from Aldrich and distilled prior to use.

Amine Syntheses. (*i*) *Synthesis of 2-(2-Methoxy)ethoxyethylamine (1).* Compound 1 was prepared by the methylation

(5) (a) Tonge, L. M.; Richeson, D. S.; Marks, T. J.; Zhao, J.; Zhang, J.; Wessels, B. W.; Marcy, H. O.; Kannewurf, C. R. *Adv. Chem. Ser.* **1990**, *226*, 351. (b) Rees, Jr., W. S.; Caballero, C. R.; Hesse, W. *Angew. Chem., Int. Engl. Ed.* **1992**, *31*, 735. (c) Timmer, K.; Spee, C. I. M. A.; Mackor, A.; Meinema, H. A.; Spek, A. L.; van der Sluis, P. *Inorg. Chim. Acta* **1991**, *190*, 109. (d) Gardiner, R.; Brown, D. W.; Kirlin, P. S.; Rheingold, A. L. *Chem. Mater.* **1991**, *3*, 1053.

(6) Various synthetic approaches have yielded the following crystalline compositions: (a) $Ba_5(dpm)_9(H_2O)_2(OH)$: Turnipseed, S. B.; Barkley, R. M.; Sievers, R. E. *Inorg. Chem.* **1991**, *30*, 1164. (b) [Ba(dpm)$_2$·2NH$_3$]$_2$: Rees, Jr., W. S.; Carris, M. W.; Hesse, W. *Inorg. Chem.* **1991**, *30*, 4479. (c) Ba(dpm)$_2$(CH$_3$OH)$_3$·CH$_3$OH: Gleizes, A.; Sans-Lenain, S.; Medus, D.; Morancho, R. *C.R. Acad. Sci., Ser. II Univers.* **1991**, *312*, 983. (d) [Ba(dpm)$_2$·Et$_2$O]$_2$: Rosetto, G.; Polo, A.; Benetollo, F.; Porchia, M.; Zanella, P. *Polyhedron* **1992**, *11*, 979.

(7) Addition of a Lewis bases to the carrier gas affords some improvement: (a) Dickinson, P. H.; Geballe, T. H.; Sanjurjo, A.; Hildenbrand, D.; Craig, G.; Zisk, M.; Collman, J.; Banning, S. A.; Sievers, R. E. *J. Appl. Phys.* **1989**, *66*, 444. (b) Matsuno, S.; Uchikawa, F.; Yoshizaki, K. *Jap. J. Appl. Phys.* **1990**, *29*, L947. (c) Zhang, J. M.; DiMeo, Jr., F.; Wessels, B. W.; Schulz, D. L.; Marks, T. J.; Schindler, J. L.; Kannewurf, C. R. *J. Appl. Phys.* **1992**, *71*, 2769. (d) Barron, A. R. *Strem Chem.* **1990**, *13*, 1.

(8) Chakravorty, A.; Fennessey, J. P.; Holm, R. H. *Inorg. Chem.* **1965**, *4*, 26.

(9) Panson, A. J.; Charles, R. G.; Schmidt, D. N.; Szedon, J. R.; Machiko, G. J.; Braginski, A. I. *Appl. Phys. Lett.* **1988**, *53*, 1756.

(10) (a) Fu, W. T.; Zandbergen, H. W.; Xu, Q.; van Ruitenceek, J. M.; de Jongh, L. J.; van Tendeloo, G. *Solid State Commun.* **1989**, *70*, 1117. (b) Shannon, R. D.; Bierstedt, P. E. *J. Am. Ceram. Soc.* **1970**, *53*, 635.

(11) Swarmer, F. W.; Hauser, C. R. *J. Am. Chem. Soc.* **1950**, *72*, 1352.

of 2-(2-aminoethoxy)ethanol. A 1-L flask containing 600 mL of THF was charged under inert atmosphere with 12.61 g of NaH (525 mmol) and cooled in an ice bath. Under an inert atmosphere, 2-(2-aminoethoxy)ethanol (51.48 g, 490 mmol) was added dropwise with stirring over the course of 20 min. The ice bath was then removed, and the resulting white slurry stirred for about 2 h until H_2(g) liberation had ceased. An ice bath was next employed, and 74.63 g of CH_3I (526 mmol) was added dropwise with stirring over the course of 3 min, giving a cider-colored solution. After 1 h of stirring, the solvent was removed in vacuo. The remaining slurry was distilled twice giving 44.85 g (77% yield) of colorless liquid 1: bp 30–35 °C/0.01 Torr; ^{1}H NMR (300 MHz, $CDCl_3$) δ 1.16 (br s, 2H), 2.73 (m, 2H), 3.25 (s, 3H), 3.37 (m, 2H), 3.42 (m, 2H), 3.47 (m, 2H). Anal. Calcd for $C_5H_{13}NO_2$: C, 50.40; H, 11.00; N, 11.75. Found: C, 50.67; H, 11.26; N, 11.52.

(*ii*) *Synthesis of 2-(2-Ethoxy)ethyl Tosylate* (*2*). Under an inert atmosphere, a 2-L flask containing 1 L of dry pyridine was charged with 91.47 g of 2-ethoxyethanol (1.015 mol) and the mixture was cooled to 0 °C using an ice bath. Next, *p*-toluenesulfonyl chloride (193.68 g, 1.016 mol) was added with stirring. The reaction mixture was then stirred for 19 h as the ice bath warmed to room temperature. The reaction mixture was next quenched with 1 L of ice and acidified to pH ~ 2 with concentrated hydrochloric acid. The aqueous phase was extracted with 3 × 500 mL of diethyl ether, and the combined extracts were then dried over Na_2SO_4. After filtration, the diethyl ether was removed in vacuo, affording 175.9 g (71% yield) of **2** as a yellow oil. ^{1}H NMR (300 MHz, $CDCl_3$): δ 1.07 (m, 3H), 2.38 (s, 3H), 3.38 (m, 2H), 3.54 (m, 2H), 4.09 (m, 2H), 7.27 (s, 1H), 7.30 (s, 1H), 7.73 (s, 1H), 7.75 (s, 1H). Anal. Calcd for $C_{13}H_{16}SO_4$: C, 54.08; H, 6.60. Found: C, 54.18; H, 7.00.

(*iii*) *Synthesis of 2-(2-(2-Ethoxy)ethoxy)ethoxyethylamine* (*3*). A 2-L flask containing 500 mL of THF was charged under inert atmosphere with 5.54 g of NaH (231 mmol). After the flask was cooled in an ice bath, 2-(2-aminoethoxy)ethanol (24.16 g, 230 mmol) was added dropwise with stirring over the course of 3 min. The reaction mixture was then stirred for 1 additional hour at which time H_2 liberation had ceased. Next, **2** (56.12 g, 230 mmol) was added dropwise with stirring over the course of 10 min. The reaction mixture was then stirred for 12 h as the ice bath warmed. The reaction mixture was suction filtered and the solvent removed in vacuo. The liquid remaining was vacuum distilled giving 25.98 g (64% yield) of a colorless liquid identified as **3**: bp 75–80 °C/0.01 Torr; ^{1}H NMR (300 MHz, $CDCl_3$) δ 1.11 (m, 3H), 1.62 (br s, 2H), 2.76 (m, 2H), 3.42 (m, 4H), 3.49 (m, 2H), 3.55 (m, 6H). Anal. Calcd for $C_8H_{19}NO_3$: C, 54.21; H, 10.81; N, 7.90. Found: C, 52.24; H, 10.78; N, 7.85.

β-Ketoimine Syntheses. β-Ketoimines derived from 2,2-dimethyl-3,5-hexanedione were prepared by condensation of the β-diketone with the corresponding amino ethers in benzene.[12] β-Ketoimines derived from 2,2,6,6-tetramethyl-3,5-heptanedione (Hdpm) were prepared by reaction of the corresponding amino ether with the trimethylsilyl enol ether derivative of Hdpm following the general method of Shin, et al.[13]

(*i*) *Synthesis of 2,2-Dimethyl-5-N-(2-methoxyethylimino)-3-hexanone* [*Hmiki*] (*4*). To 200 mL of benzene was added 2,2-dimethyl-3,5-hexanedione (9.14 g, 6.4 mmol) and 4.83 g of 2-methoxyethylamine (6.4 mmol) under an inert atmosphere. Next, 0.7 mL of glacial acetic acid catalyst was added, and a Dean-Stark trap equipped with a drying tube was employed to azeotrope water from the refluxing reaction mixture. The reaction mixture was refluxed with vigorous stirring for 6 h at which time a yellow color was observed. The solvent was next removed in vacuo and the residual liquid was subjected to vacuum distillation, affording 11.62 g (91% yield) of low-melting yellow solid (mp 40 °C) identified as **4**: bp 85–90 °C/0.05 Torr; ^{1}H NMR (300 MHz, $CDCl_3$) δ 1.09 (s, 9H), 1.94 (s, 3H), 3.33 (s, 3H), 3.39 (m, 2H), 3.48 (m, 2H), 5.11 (s, 1H), 10.94 (br s, 1H); ^{13}C NMR (75 MHz, $CDCl_3$) δ 201.25 [*C*O], 161.95 [*C*N], 88.87 [*C*H], 70.20 [*OCH*$_2$], 57.22 [*OCH*$_3$], 41.40 [*NCH*$_2$], 39.59 [*C*(CH$_3$)$_3$], 26.54 [C(*CH*$_3$)$_3$], 17.81 [CNCH$_3$]. Anal. Calcd for $C_{11}H_{21}NO_2$: C, 66.29; H, 10.62; N, 7.03. Found: C, 66.56; H, 10.72; N, 7.19. MS (EI, 70 eV, *m/e*+; (fragment); HL = Hmiki) 199 (HL), 154 (HL – CH_2OCH_3), 142 (HL – C_4H_9), 83 (HL – C_4H_9 – $C_2H_4OH_3$), 59 ($C_2H_4OCH_3$), 57 (C_4H_9).

(*ii*) *Synthesis of 2,2-Dimethyl-5-N-(2-(2-methoxy)ethoxyethylimino)-3-hexanone* [*Hdiki*] (*5*). This β-ketoimine was prepared analogously to **4**, starting from 19.78 g of 2,2-dimethyl-3,5-hexanedione (139 mmol) and 16.58 g of **1** (139 mmol). Vacuum distillation afforded 25.00 g (74% yield) yellow liquid identified as **5**: bp 110–112 °C/0.01 Torr; ^{1}H NMR (300 MHz, $CDCl_3$) δ 1.06 (s, 9H), 1.97 (s, 3H), 3.29 (s, 3H), 3.43 (m, 2H), 3.49 (m, 2H), 3.58 (m, 4H), 5.13 (s, 1H), 11.01 (br s, 1H); ^{13}C NMR (75 MHz, $CDCl_3$) δ 203.61 [*C*O], 163.59 [*C*N], 90.56 [*C*H], 71.69 [*OCH*$_2$], 70.48 [*OCH*$_2$], 70.21 [*CH*$_2$*OCH*$_3$], 58.85 [*OCH*$_3$], 42.77 [*NCH*$_2$], 41.03 [*C*(CH$_3$)$_3$], 27.76 [C(*CH*$_3$)$_3$], 19.28 [CNCH$_3$]. Anal. Calcd for $C_{13}H_{25}NO_3$: C, 64.16; H, 10.36; N, 5.76. Found: C, 63.84; H, 10.34; N, 5.75. MS (EI, 70 eV, *m/e*+; (fragment); HL = Hdiki) 243 (HL), 186 (HL – C_4H_9), 154 (HL – $CH_2OC_2H_4OCH_3$), 110 (HL – C_4H_9 – $OC_2H_4OCH_3$), 82 (HL – C_4H_9 – CH_3 – $CH_2OC_2H_4OCH_3$), 59 ($C_2H_4OCH_3$), 57 (C_4H_9), 45 (CH_2OCH_3).

(*iii*) *Synthesis of 2,2-Dimethyl-5-N-(2-(2-(2-ethoxy)ethoxy)ethoxyethylimino)-3-hexanone* [*Htriki*] (*6*). This β-ketoimine was prepared analogously to **4**, starting from 8.92 g of 2,2-dimethyl-3,5-hexanedione (63 mmol) and 11.12 g of **3** (63 mmol). Vacuum distillation afforded 13.50 g (71% yield) of yellow liquid which was identified as **6**: bp 145–150 °C/0.01 Torr; ^{1}H NMR (300 MHz, $CDCl_3$) δ 1.07 (s, 9H), 1.15 (m, 3H), 1.92 (s, 3H), 3.39–3.60 (m, 14H), 5.08 (s, 1H), 10.93 (br s, 1H); ^{13}C NMR (75 MHz, $CDCl_3$) δ 203.71 [*C*O], 163.69 [*C*N], 90.64 [*C*H], 72.79 [*OCH*$_2$], 70.69 [*OCH*$_2$], 70.62 [*OCH*$_2$], 70.47 [*OCH*$_2$], 70.30 [*OCH*$_2$], 69.75 [*OCH*$_2$], 66.51 [*NCH*$_2$], 42.90 [*C*(CH$_3$)$_3$], 27.86 [C(*CH*$_3$)$_3$], 19.40 [CNCH$_3$], 15.08 [CH$_2$*CH*$_3$]. Anal. Calcd for $C_{16}H_{31}NO_4$: C, 63.76; H, 10.37; N, 4.65. Found: C, 62.93; H, 10.55; N, 4.83. MS (EI, 70 eV, *m/e*+; (fragment); HL = Htriki) 301 (HL), 244 (HL – C_4H_9), 171 (HL – C_4H_9 – $C_2H_4OC_2H_5$), 73 ($C_2H_4OC_2H_5$), 57 (C_4H_9), 45 (OC_2H_5).

(*iv*) *Synthesis of 2,2,6,6-Tetramethyl-5-(trimethylsiloxy)hept-4-en-3-one* (*7*). Under an inert atmosphere, NaH (7.00 g, 292 mmol) was suspended in 600 mL of diethyl ether in a silated 1-L Schlenk flask, and the reaction mixture was cooled to 0 °C with an ice bath. Hdpm (50.12 g, 272 mmol) was then added dropwise to the solution with stirring over a period of 45 min, yielding a cider-brown solution. Chlorotrimethylsilane (31.70 g, 292 mmol) was then added dropwise over 10 min. Next, a condenser was attached and the mixture was refluxed for 40 h. The reaction mixture was then filtered through Celite giving a colorless solution. The diethyl ether was removed in vacuo at 0 °C giving 43.08 g (62 % yield) of 96% pure **7** (4% 2,2,6,6-tetramethyl-3,5-heptanedione impurity, by ^{1}H NMR integration). This reagent was sufficiently pure for subsequent syntheses. ^{1}H NMR (300 MHz, $CDCl_3$) δ 0.24 (s, 9H), 1.09 (s, 18H), 5.80 (s, 1H). Anal. Calcd for $C_{14}H_{28}SiO_2$: C, 65.57; H, 11.01. Found: C, 65.22; H, 10.78.

(*v*) *Synthesis of 5-N-(2-Methoxyethylimino)-2,2,6,6-tetramethyl-3-heptanone* [*Hdpmiki*] (*8*). Under inert atmosphere, **7** (15.69 g, 61 mmol) and 2-methoxyethylamine (5.02 g, 67 mmol) were heated in a silated 250-mL Schlenk flask with vigorous stirring at 90–95 °C for 3 h. The reaction mixture was then vacuum distilled twice affording 5.39 g (37% yield) yellow liquid which was identified as **8**: bp 90–92 °C/0.01 Torr; ^{1}H NMR (300 MHz, $CDCl_3$) δ 1.12 (s, 9H), 1.26 (s, 9H), 3.38 (s, 3H), 3.55 (m, 2H), 3.63 (m, 2H), 5.30 (s, 1H), 10.62 (br s, 1H); ^{13}C NMR (75 MHz, $CDCl_3$) δ 203.58 [*C*O], 173.30 [*C*N], 86.50 [*C*H], 71.44 [*OCH*$_2$], 58.48 [*OCH*$_3$], 44.96 [*NCH*$_2$], 41.56 [*COC*(CH$_3$)$_3$], 35.82 [*CNC*(CH$_3$)$_3$], 28.94 [COC(*CH*$_3$)$_3$], 27.94 [CNC(*CH*$_3$)$_3$]. Anal. Calcd for $C_{14}H_{27}NO_2$: C, 69.67; H, 11.28; N, 5.80. Found: C, 69.85; H, 11.01; N, 5.92. MS: (EI, 70 eV, *m/e*+; (fragment); HL = Hdpmiki) 241 (HL), 226 (HL – CH_3), 198 (HL – $C_2H_4OCH_3$), 184 (HL – C_4H_9), 68 (HL – C_4H_9 – CH_3 – $C_2H_4OCH_3$), 59 ($C_2H_4OCH_3$), 57 (C_4H_9).

(*vi*) *Synthesis of 5-N-(2-(2-Methoxy)ethoxyethylimino)-2,2,6,6-tetramethyl-3-heptanone* [*Hdpdiki*] (*9*). Under inert atmosphere, **7** (16.81 g, 66 mmol) and **1** (8.53 g, 72 mmol) were heated in a silated 250-mL Schlenk flask at 110 °C for 3 h with vigorous stirring. The reaction mixture was then vacuum distilled twice affording 5.10 g (27% yield) yellow liquid which was identified as **9**: bp 110–115 °C/0.01 Torr; ^{1}H NMR (300 MHz, $CDCl_3$) δ 1.08 (s, 9H), 1.22 (s, 9H), 3.32 (s, 3H), 3.51 (m, 2H),

(12) Moffett, R. B.; Hoehn, W. M. *J. Am. Chem. Soc.* **1947**, *69*, 1792.
(13) Shin, H.-K.; Hampden-Smith, M. J.; Kodas, T. T.; Rheingold, A. L. *J. Chem. Soc., Chem. Commun.* **1992**, 217.

3.58–3.64 (m, 6H), 5.26 (s, 1H), 11.58 (br s, 1H); ^{13}C NMR (75 MHz, $CDCl_3$) δ 203.13 [CO], 173.08 [CN], 86.16 [CH], 71.39 [OCH_2], 70.18 [OCH_2], 69.97 [OCH_2], 58.48 [OCH_3], 44.71 [NCH_2], 41.26 [$COC(CH_3)_3$, 35.57 [$CNC(CH_3)_3$], 28.69 [$COC(CH_3)_3$], 27.69 [$CNC(CH_3)_3$]. Anal. Calcd for $C_{16}H_{31}NO_3$: C, 67.33; H, 10.95; N, 4.91. Found: C, 66.80; H, 11.07; N, 4.87. MS: (EI, 70 eV, *m/e*+; (fragment); HL = Hdpdiki) 285 (HL), 270 (HL – CH_3), 228 (HL – C_4H_9), 196 (HL – C_4H_9 – OCH_3), 170 (HL – C_4H_9 – $C_2H_4OCH_3$), 125 (HL – C_4H_9 – $C_2H_4OC_2H_4OCH_3$), 103 ($C_2H_4OC_2H_4OCH_3$), 59 ($C_2H_4OCH_3$), 57 (C_4H_9).

(vii) Synthesis of 5-N-(2-(2-(2-Ethoxy)ethoxy)ethoxyethylimino)-2,2,6,6-tetramethyl-3-heptanone [Hdptriki] (10). This β-ketoimine was prepared analogously to **9**, starting from 10.58 g of **7** (41 mmol) and 8.03 g of **3** (45 mmol). The reaction mixture was vacuum distilled twice affording 5.74 g (41% yield) of a yellow liquid which was identified as **10**: bp 125–130 °C/0.01 Torr; ^{1}H NMR (300 MHz, $CDCl_3$) δ 1.05 (s, 9H), 1.11 (m, 3H), 1.19 (s, 9H), 3.43 (m, 2H), 3.48 (m, 2H), 3.54–3.58 (m, 10H), 5.22 (s, 1H), 11.55 (br s, 1H); ^{13}C NMR (75 MHz, $CDCl_3$) δ 203.67 [CO], 173.54 [CN], 86.58 [CH], 70.68 [OCH_2], 70.58 [OCH_2], 70.40 [OCH_2], 70.30 [OCH_2], 69.72 [OCH_2], 66.46 [OCH_2], 45.08 [NCH_2], 41.67 [$COC(CH_3)_3$], 35.96 [$CNC(CH_3)_3$], 29.07 [$COC(CH_3)_3$], 28.04 [$CNC(CH_3)_3$], 14.05 [CH_2CH_3]. Anal. Calcd for $C_{19}H_{37}NO_4$: C, 66.43; H, 10.86; N, 4.08. Found: C, 66.12; H, 10.44; N, 4.32. MS (EI, 70 eV, *m/e*+; (fragment); HL = Hdptriki) 343 (HL), 328 (HL – CH_3), 286 (HL – C_4H_9), 161 ($C_2H_4OC_2H_4OC_2H_4OC_2H_5$), 153 (HL – C_4H_9 – $OC_2H_4OC_2H_4OC_2H_5$), 125 (HL – C_4H_9 – $C_2H_4OC_2H_4OC_2H_4OC_2H_5$), 117 ($C_2H_4OC_2H_4OC_2H_5$), 73 ($C_2H_4OC_2H_5$), 57 ($C_4H_9$), 45 ($OC_2H_5$).

Barium β-Ketoiminate Syntheses. *(i) Synthesis of Bis[2,2-dimethyl-5-N-(2-methoxyethylimino)-3-hexanonato]barium-(II) {[Ba(miki)$_2$]$_2$} (11).* BaH_2 (1.60 g, 12 mmol) was weighed into a Schlenk frit assembly. Next, **4** (3.68 g, 19 mmol) was syringed in under an N_2 purge. The reaction mixture was stirred and heated to 110 °C for 2 h after which time a yellow solid formed. Heptane (50 mL) was then added and the mixture was heated to reflux. The resulting solution was filtered hot and allowed to slowly cool to room temperature at which time a yellow solid formed. The heptane was then removed in vacuo, and the remaining solid was dissolved in 5 mL of pentane. The resulting solution was placed in a –20 °C freezer for several days at which time a white crystalline material had settled to the bottom of the flask. The yellow mother liquor was decanted off, and the remaining solid was dried in vacuo giving 2.39 g (49 % yield) **11**: mp 138–140 °C; ^{1}H NMR (300 MHz, C_6D_6) δ 1.41 (s, 9 H), 1.80 (s, 3H), 3.10 (s, 3H), 3.20 (m, 2H), 3.56 (m, 2H), 5.10 (s, 1H); ^{13}C NMR (75 MHz, C_6D_6) δ 186.54 [CO], 104.73 [CN], 92.80 [CH], 74.16 [OCH_2], 58.65 [OCH_3], 49.41 [NCH_2], 39.77 [$C(CH_3)_3$], 29.81 [$C(CH_3)_3$], 21.47 [$CNCH_3$]. Anal. Calcd for $C_{22}H_{40}N_2O_4Ba$: C, 49.49; H, 7.55; N, 5.25. Found: C, 49.24; H, 7.96; N, 5.12. TGA (49.61 mg) T_{50} = 299 °C; 39% residue to 500 °C. MS (EI, 70 eV, *m/e*+; (fragment); M = Ba(miki)$_2$, L = miki) 534 (M), 503 (M – OCH_3), 472 (M – $2OCH_3$), 336 (M – L), 305 (M – L – OCH_3), 167 (L – OCH_3), 141 (L – C_4H_9).

(ii) Synthesis of Bis[2,2-dimethyl-5-N-(2-(2-methoxy)ethoxyethylimino)-3-hexanonato]barium(II) [Ba(diki)$_2$] (12). This barium complex was prepared analogously to **11** starting with 1.39 g of BaH_2 (10 mmol) and 4.80 g of **5** (20 mmol). The reaction mixture was stirred for 1 h at 100 °C after which time a yellow solid formed. The solid was recrystallized repeatedly from hot heptane until the mother liquor was colorless giving 2.70 g (44% yield) of **12**: mp 170–171 °C; ^{1}H NMR (300 MHz, C_6D_6), δ 1.43 (s, 9H), 1.82 (s, 3H), 3.03 (s, 3H), 3.07 (m, 2H), 3.29 (m, 2H), 3.39 (m, 2H), 3.66 (m, 2H), 5.10 (s, 1H); ^{13}C NMR (75 MHz, C_6D_6) δ 186.03 [CO], 167.82 [CN], 91.63 [CH], 72.97 [OCH_2], 71.59 [OCH_2], 69.47 [OCH_2], 58.51 [OCH_3], 51.32 [NCH_2], 39.85 [$C(CH_3)_3$], 30.05 [$C(CH_3)_3$], 22.38 [$CNCH_3$]. Anal. Calcd for $C_{26}H_{48}N_2O_6Ba$: C, 50.21; H, 7.78; N, 4.50; Ba, 22.08. Found: C, 49.30; H, 7.72; N, 4.26; Ba, 22.26. TGA (52.05 mg) T_{50} = 278 °C; 39% residue to 500 °C. MS (EI, 70 eV, *m/e*+; (fragment); M = Ba(diki)$_2$, L = diki) 622 (M), 607 (M – CH_3), 546 (M – $OCH_2H_4OCH_3$), 470 (M – $2OC_2H_4OCH_3$ – $2CH_3$), 380 (M – L), 304 (M – L – $OC_2H_4OCH_3$), 185 (L – C_4H_9).

(iii) Synthesis of Bis[2,2-Dimethyl-5-N-(2-(2-(2-ethoxy)-ethoxy)ethoxyethylimino)-3-hexanonato]barium(II) [Ba(triki)$_2$] (13). This barium complex was prepared analogously to **11**, starting with 1.25 g of BaH_2 (9 mmol) and 5.41 g of **6** (18 mmol). The reaction mixture was stirred for 1 h at 140 °C after which time a yellow solid formed. The solid was recrystallized repeatedly from hot heptane until the mother liquor was colorless, giving 2.83 g (42% yield) of **13**: mp 80–82 °C; ^{1}H NMR (300 MHz, C_6D_6) δ 1.12 (m, 3H), 1.44 (s, 9H), 1.83 (s, 3H), 3.36–3.59 (m, 14H), 5.08 (s, 1H); ^{13}C NMR: (300 MHz, C_6D_6): δ 186.08 [CO], 167.22 [CN], 91.55 [CH], 72.75 [OCH_2], 70.31 [OCH_2], 70.13 [OCH_2], 69.69 [OCH_2], 69.45 [OCH_2], 66.41 [CH_2CH_3], 50.61 [NCH_2], 39.89 [$C(CH_3)_3$], 30.10 [$C(CH_3)_3$], 22.18 [$CNCH_3$], 15.32 [CH_2CH_3]. Anal. Calcd for $C_{32}H_{60}N_2O_8Ba$: C, 52.07; H, 8.19; N, 3.80; Ba, 18.60. Found: C, 51.55; H, 8.38; N, 3.47; Ba, 18.27. TGA (52.00 mg) T_{50} = 255 °C; 29% residue to 500 °C. MS (EI, 700 eV, *m/e*+; (fragment); M = Ba(triki)$_2$, L = triki) 738 (M), 723 (M – CH_3), 681 (M – C_4H_9), 604 (M – $C_2H_4OC_2H_4OC_2H_5$), 438 (M – L), 243 (L – C_4H_9).

(iv) Synthesis of Bis[5-N-(2-methoxyethylimino)-2,2,6,6-tetramethyl-3-heptanonato]barium(II) [{Ba(dpmiki)$_2$}$_2$] (14). This barium complex was prepared analogously to **11**, starting with 1.84 g of BaH_2 (13 mmol) and 5.39 g of **8** (22 mmol). The reaction mixture was stirred for 24 h at 95 °C, after which time a yellow solid formed. The solid was recrystallized repeatedly from hot heptane until the mother liquor was colorless, giving 3.71 g (54% yield) of **14**: mp 165–168 °C; ^{1}H NMR (300 MHz, C_6D_6, major isomer) δ 1.17 (s, 9H), 1.41 (s, 9H), 3.11 (s, 3H), 3.38 (m, 2H), 3.54 (m, 2H), 5.33 (s, 1H); ^{13}C NMR (75 MHz, C_6D_6, major isomer) δ 187.64 [CO], 181.62 [CN], 84.08 [CH], 74.21 [OCH_2], 58.64 [OCH_3], 49.35 [NCH_2], 40.57 [$C(CH_3)_3$], 40.02 [$C(CH_3)_3$], 30.06 [$C(CH_3)_3$], 29.74 [$C(CH_3)_3$]. Anal. Calcd for $C_{28}H_{52}N_2O_4Ba$: C, 54.41; H, 8.48; N, 4.53. Found: C, 54.19; H, 8.87; N, 4.74. TGA (47.56 mg) T_{50} = 247 °C; 33% residue to 500 °C. MS (EI, 70 eV, *m/e*+; (fragment); M = Ba(dpmiki)$_2$, L = dpmiki) 618 (M), 603 (M – CH_3), 587 (M – OCH_3), 561 (M – C_4H_9), 559 (M – $C_2H_4OCH_3$), 504 (M – $2C_4H_9$), 378 (M – L), 347 (M – L– OCH_3), 319 (M – L – $C_2H_4OCH_3$), 262 (M – L – $C_2H_4OCH_3$ – C_4H_9), 183 (L – C_4H_9), 59 ($C_2H_4OCH_3$), 57 (C_4H_9).

(v) Synthesis of Bis[5-N-(2-(2-methoxy)ethoxyethylimino)-2,2,6,6-tetramethyl-3-heptanonato]barium(II) [Ba(dpdiki)$_2$] (15). This barium complex was prepared analogously to **11**, starting with 1.88 g of BaH_2 (13 mmol) and 5.10 g of **9** (18 mmol). The reaction mixture was stirred for 24 h at 105 °C after which time a yellow solid formed. The solid was recrystallized repeatedly from hot heptane until the mother liquor was colorless, giving 2.84 g (45% yield) of **15**: mp 137–139 °C; ^{1}H NMR (300 MHz, C_6D_6, major isomer) δ 1.44 (s, 9H), 1.46 (s, 3H), 3.07 (m, 2H), 3.13 (m, 2H), 3.21 (m, 2H), 3.43 (s, 3H), 3.57 (m, 2H), 5.26 (s, 1H); ^{13}C NMR (75 MHz, C_6D_6, major isomer) δ 189.41 [CO], 182.09 [CN], 84.34 [CH], 74.83 [OCH_2], 70.48 [OCH_2], 69.73 [OCH_2], 59.42 [OCH_3], 50.49 [NCH_2], 40.48 [$C(CH_3)_3$], 39.19 [$C(CH_3)_3$], 30.04 [$C(CH_3)_3$], 29.47 [$C(CH_3)_3$]. Anal. Calcd for $C_{32}H_{60}N_2O_6Ba$: C, 54.43; H, 8.56; N, 3.97. Found: C, 54.24; H, 8.55; N, 3.63. TGA (63.23 mg) T_{50} = 276 °C; 26% residue to 500 °C. MS (EI, 70 eV, *m/e*+; (fragment); M = Ba(dpdiki)$_2$, L = dpdiki) 706 (M), 648 (M – C_4H_9), 631 (M – $OC_2H_4OCH_3$), 422 (M – L), 284 (L), 227 (L – C_4H_9), 103 ($C_2H_4OC_2OCH_3$), 59 ($C_2H_4OCH_3$), 57 (C_4H_9), 45 (CH_2OCH_3).

(vi) Synthesis of Bis[5-N-(2-(2-(2-ethoxy)ethoxy)ethoxyethylimino)-2,2,6,6-tetramethyl-3-heptanonato]barium(II) [Ba(dptriki)$_2$] (16). This barium complex was prepared analogously to **11**, starting with 1.60 g of BaH_2 (12 mmol) and 5.74 g of **10** (17 mmol). The reaction mixture was stirred for 24 h at 95 °C after which time a yellow solid formed. The solid was recrystallized repeatedly from hot heptane until the mother liquor was colorless, giving 4.86 g (71% yield) of **16**: mp 127–128 °C; ^{1}H NMR (300 MHz, C_6D_6, major isomer) δ 1.10 (m, 3H), 1.46 (s, 9H), 1.51 (s, 3H), 3.24 (m, 2H), 3.36 (m, 2H), 3.42 (m, 4H), 3.54 (m, 2H), 3.86 (m, 2H), 4.08 (m, 2H), 5.28 (s, 1H); ^{13}C NMR (75 MHz, C_7D_8, major isomer) δ 186.46 [CO], 179.49 [CN], 83.56 [CH], 76.17 [OCH_2], 70.28 [OCH_2], 69.40 [OCH_2], 67.78 [OCH_2], 66.54 [OCH_2], 49.85 [NCH_2], 40.27 [$C(CH_3)_3$], 39.09 [$C(CH_3)_3$], 30.40 [$C(CH_3)_3$], 29.95 [$C(CH_3)_3$], 14.32 [CH_2CH_3]. Anal. Calcd for $C_{38}H_{72}N_2O_8Ba$: C, 55.50; H, 8.83; N, 3.41. Found: C, 55.49; H, 8.83; N, 3.41. TGA (47.73 mg) T_{50} = 271 °C; 23% residue to 500 °C. MS (EI, 70 eV, *m/e*+; (fragment); M = Ba(dptriki)$_2$, L = dptriki) 822 (M), 807 (M – CH_3), 689 (M – $OC_2H_4OC_2H_4OC_2H_5$), 480 (M – L), 285 (L – C_4H_9), 117 ($C_2H_4OC_2H_4OC_2H_5$), 73 ($C_2H_4OC_2H_5$), 59 ($CH_2OC_2H_5$), 57 (C_4H_9), 45 (OC_2H_5).

Single-Crystal X-ray Diffraction Studies. X-ray data for a single crystals of $Ba(diki)_2$ (**12**), $Ba(triki)_2$ (**13**), and $\{Ba(dpmiki)_2\}_2$ (**14**) (grown from heptane solution and mounted on a glass fiber with Paratone-N (Exxon) at −120 °C) were collected on an Enraf-Nonius CAD4 with graphite-monochromated Mo Kα radiation. For **12**, **13**, and **14**, cell constants and an orientation matrix for data collection, obtained from a least-squares refinement using the setting angles of 25 carefully centered reflections in the range $19.9 < 2\theta < 21.9°$, $19.2 < 2\theta < 24.1°$, and $19.5 < 2\theta < 21.9°$, respectively, corresponded to a monoclinic, an orthorhombic, and a monoclinic cell with dimensions listed in Table I. The following systematic absences were observed for **12**, **13**, and **14**, respectively, hkl ($h + k \neq 2n$) and $h0l$ ($l \neq 2n$); $0kl$ ($l \neq 2n$), $h0l$ ($l \neq 2n$) and $hk0$ ($h + k \neq 2n$); and hkl ($h + k \neq 2n$) and $h0l$ ($l \neq 2n$). On the basis of packing considerations, a statistical analysis of intensity distribution, and the successful solution and refinement of the structures, the space groups of **12**, **13**, and **14** were determined to be $C2/c$ (No. 15), $Pccn$ (No. 56), and $C2/c$ (No. 15), respectively.

Diffraction data for **12**, **13**, and **14** were collected at a temperature of −120 ± 1 °C using the ω–θ scan technique to maximum 2θ values of 50.0, 52.0, and 52.0°, respectively. ω scans of several intense reflections, made prior to data collection, had an average width at half-height of 0.30, 0.20, and 0.30 ° for **12**, **13**, and **14** with a takeoff angle of 2.8°. Scans of (1.00 + 0.35 tan θ)° were made at speeds ranging from 3.0 to 15.0°/min (in ω). Moving-crystal moving counter background measurements were made by scanning an additional 25% above and below the scan range. The counter aperture consisted of a variable horizontal slit with a width ranging from 2.0 to 2.5 mm and a vertical slit set to 2.0 mm. The diameter of the incident beam collimator was 0.7 mm, and the crystal-to-detector distance was 21 cm. For intense reflections an attenuator was automatically inserted in front of the detector.

Of the 5849, 4401, and 7016 reflections which were collected for **12**, **13**, and **14**, 5627 (R_{int} = 0.064), 4157 (R_{int} = 0.038), and 6728 (R_{int} = 0.074), respectively, were unique. The intensities of three representative reflections which were measured after every 90 min of X-ray exposure time remained constant throughout data collection indicating crystal and electronic stability (no decay correction was applied). The linear absorption coefficient for Mo Kα is 13.4, 10.9, and 12.6 cm^{-1} for **12**, **13**, and **14**, respectively. An analytical absorption correction was applied which resulted in transmission factors ranging from 0.79 to 0.88 for **12**, 0.82 to 0.85 for **13**, and 0.60 to 0.83 for **14**. The data were corrected for Lorentz and polarization effects. A correction for secondary extinction was applied for **13** and **14** (coefficient = 0.16385*E*–06 and 0.18779*E*–07, respectively).

All calculations were performed using the TEXSAN crystallographic software package of Molecular Structure Corp., while pictorial representations were generated using the ORTEP program. The structures were solved by either direct methods (**12** and **13**) or a combination of the Patterson method and direct methods (**14**), (SHELXS-86). All non-hydrogen atoms were refined anisotropically. The hydrogen atoms in **12** and **13** were refined with a group isotropic thermal parameter while the hydrogen atoms for **14** were included as fixed contributors in "idealized" positions. One hydrogen atom in **12** (20A) was assigned a fixed geometry due to minor disorder. The final cycle of full-matrix least-squares refinements for **12**, **13**, and **14** were based on 2776, 1689, and 4881 observed reflections ($I > 3.00\sigma(I)$) and 458, 286, and 345 variable parameters, respectively. The refinements for **12**, **13**, and **14** converged (largest parameter shift was 0.41, 0.07, and 0.59 times its esd, respectively) with unweighted and weighted agreement factors of $R = \sum||F_o| - |F_c||/\sum|F_o|$ = 0.044, 0.036, and 0.033 and $R_W = [(\sum W(|F_o| - |F_c|)^2/\sum wF_o^2)]^{1/2}$ = 0.040, 0.035, and 0.042, respectively. The standard deviation of an observation of unit weight for **12**, **13**, and **14** was 1.15, 1.11, and 1.76, respectively. The weighting scheme was based on counting statistics and included a factor (p = 0.03) to downweight the intense reflections. Plots of $\sum w(|F_o| - |F_c|)^2$ versus $|F_o|$, reflection order in data collection, $\sin\theta/\lambda$, and various classes of indices showed no unusual trends. The maximum and minimum peaks on the final difference Fourier maps for **12**, **13**, and **14** corresponded to 0.65 and −0.67, 0.56, and −0.66, and 1.00 and −0.69 e$^-$/Å, respectively. The highest peaks left in the difference map of **14** were in the vicinity of the barium position.

Table I. Crystal Data and Diffraction Experimental Details for Barium Ketoiminate Complexes.

	12	**13**	**14**
formula	$C_{26}H_{48}N_2O_6Ba$	$C_{32}H_{60}N_2O_6Ba$	$C_{28}H_{52}N_2O_4Ba$
fw	622.01	738.16	618.06
space group	$C2/c$ (No. 15)	$Pccn$ (No. 56)	$C2/c$ (No. 15)
a, Å	32.764(6)	24.939(4)	27.687(5)
b, Å	12.110(2)	10.546(2)	10.453(2)
c, Å	15.690(5)	14.349(4)	22.679(6)
β, deg	102.12(2)		101.88(2)
V, Å^3	6087(4)	3774(2)	6423(4)
Z	8	4	8
temp, °C	−120 ± 1	−120 ± 1	−120 ± 1
d_{calc}, g/cm^3	1.357	1.299	1.278
λ(Mo Kα) radiation, Å	0.710 69	0.710 69	0.710 69
μ, cm^{-1}	13.39	10.94	12.64
transm factors	0.79–0.88	0.82–0.85	0.60–0.83
R^a	0.044	0.036	0.033
$R_w{}^b$	0.040	0.035	0.042

$^a R = \sum||F_o| - |F_c||/\sum|F_o|$. $^b R_w = [(\sum w(|F_o| - |F_c|)^2/\sum w|F_o|^2)]^{1/2}$.

For **14**, there is a disorder in C5, C6, and C7 (*tert*-butyl) methyl groups which were set to equal full occupancy with their counter B group. The B group refined to an occupancy of 0.56. Crystallographic details are collected in Table I.

MOCVD Experiments and $BaPbO_3$ Film Characterization. Preliminary studies of $BaPbO_3$ film growth were carried out in a horizontal quartz, low-pressure, hot-wall reactor of conventional design. The precursors $Ba(diki)_2$ (**12**) and $Pb(dpm)_2$[14] were used as the Ba and Pb sources, respectively. They were contained in resistively heated alumina boats (180 and 125 °C, respectively) and were transported to the resistively heated susceptor zone with flowing Ar (200 sccm). The total system pressure was 5 Torr. Water-saturated O_2 flowing at 200 sccm was introduced into the gas stream 3 cm upstream of the susceptor. The susceptor consisted of a 1.0 cm × 1.0 cm quartz plate with an imbedded K-type thermocouple. (001) MgO substrates were first degreased by sonication in methanol for 10 min before being attached to the susceptor with graphite paint. In a typical film growth experiment, PbO_x was first deposited for 1 h at a substrate temperature of 300 °C, followed by BaO deposition for 1 h at 450 °C. The as-deposited films are amorphous by X-ray diffraction. A 10-min postanneal at 890 °C in air yielded crystalline $BaPbO_3$ films containing traces of BaO (Figure 8). The presence of the latter phase is consistent with SEM/EDX measurements which indicate that the $BaPbO_3$ films are slightly Ba-rich. Under these conditions, typical film growth rates are ca. 1–2 μm h^{-1}.

Film thickness was measured on a Tencor Instruments Alpha Step 200 profilometer. Atomic concentrations of barium and lead were monitored by scanning electron microscopy energy-dispersive X-ray spectroscopy (SEM/EDS) on a Hitachi S570-LB scanning electron microscope using a Tracor Northern TN5500 energy-dispersive spectrometer. The crystalline phase composition of the films was determined by X-ray diffraction (XRD) $\theta/2\theta$ analysis using a computer-interfaced Rigaku DMAX-A instrument with Ni-filtered Cu Kα radiation operating at 50 kV/30 mA. Four-probe resistivity data were obtained on a computer-automated charge-transport system which has been previously described.[15] Electrodes were attached to the samples with silver paint.

Results and Discussion

Ligand and Complex Synthesis. The β-ketoimine ligands **4**, **5**, and, **6** were synthesized by condensation in benzene of 2,2-dimethyl-3,5-hexanedione with the corresponding polyether amine (Scheme I). Synthesis of the Hdpm-derived β-ketoimines according to this procedure, was unsuccessful, even in higher boiling toluene, presumably due to the steric bulk of the adjacent ^{t}*Bu* group.[16] However, the β-ketoimine ligands **8**, **9**, and **10** could be

(14) Schweitzer, G. K.; Pullen, B. P.; Fang, Y. *Anal. Chim. Acta* **1968**, *43*, 332.
(15) Lyding, J. W.; Marcy, H. O.; Marks, T. J.; Kannewurf, C. R. *IEEE Trans. Instrum. Meas.* **1988**, *37*, 76.
(16) Layer, R. W. *Chem. Rev.* **1963**, *63*, 489.

Scheme I. β-Ketoimine Ligand Synthesis

β-Ketoimines based upon 2,2-dimethyl-3,5-hexanedione

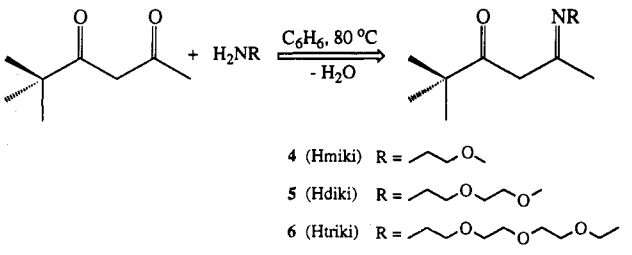

β-Ketoimines based upon 2,2,6,6-tetramethyl-3,5-heptanedione

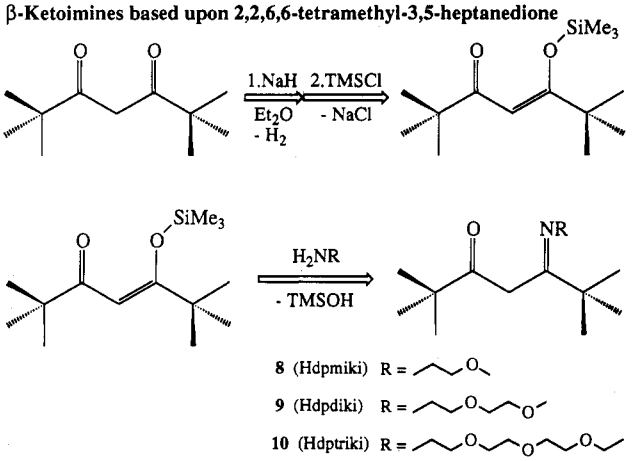

synthesized in good yields by reaction of the corresponding amino ethers with the trimethylsilyl enol ether derivative of Hdpm (Scheme I). All barium β-ketoiminate complexes were synthesized by reaction of the ligand protio derivatives with BaH_2 under inert atmosphere (eq 1). They

$$2HL + BaH_2 \xrightarrow{\Delta} BaL_2 + 2H_2 \quad (1)$$

4 (Hmiki)	11 $Ba(miki)_2$
5 (Hdiki)	12 $Ba(diki)_2$
6 (Htriki)	13 $Ba(triki)_2$
8 (Hdpmiki)	14 $\{Ba(dpmiki)_2\}_2$
9 (Hdpdiki)	15 $Ba(dpdiki)_2$
10 (Hdptriki)	16 $Ba(dptriki)_2$

were characterized by standard analytical techniques and, in several cases, by X-ray diffraction (vide infra).

Mass Spectral Data. The electron impact mass spectroscopic data for the six barium complexes show similar behavior. The major fragment observed in all cases is BaL^+, representing the loss of one ligand. Other fragments of lower abundance can be attributed to polyether scission and loss of a ^{t}Bu group from the β-ketoiminate backbone. All of these fragments exhibit an isotopic distribution pattern which agrees well with the calculated patterns. Also present at lower m/e^+ values are free ligand fragments. Although polynuclear fragments have been reported in electron impact studies of some barium β-diketonate complexes,[6a,17] no fragments with m/e^+ > parent ion were observed for any of the present β-ketoiminate complexes.

Solution-Phase Molecular Weight Determinations. The molecular weights of all six barium ketoiminates were determined under an inert atmosphere by cryoscopy in benzene. The results are shown in Table II. The following correlation can be drawn between the total number of available coordination sites on the ketoiminate ligands and the molecular complexity observed in the subsequent barium complexes: those complexes with ligands providing a maximum of six coordination sites (i.e., 11 and 14) are dimeric in benzene, while those complexes with ligands providing eight or more coordination sites (i.e., 12, 13, 15, and 16) are monomeric in benzene. Thus, 11 and 14, which are composed of a Ba^{2+} ion plus two potentially tridentate chelates exist in benzene solution as dimers, while 12, 13, 15, and 16, which consist of a Ba^{2+} ion plus two potentially tetradentate or pentadentate chelates are monomeric in benzene. These cryoscopic data are consistent with X-ray structural information for complexes 12, 13, and 14 (vide infra).

Table II. Cryoscopic Molecular Weight Data for Barium Ketoiminate Complexes in Benzene

complex	measured MW	monomer MW	molecular complexity
$\{Ba(miki)_2\}_2$ (11)	1234 ± 96	534	2.3 ± 0.2
$Ba(diki)_2$ (12)	734 ± 78	622	1.2 ● 0.1
$Ba(triki)_2$ (13)	740 ± 54	736	1.0 ± 0.1
$\{Ba(dpmiki)_2\}_2$ (14)	1288 ± 98	618	2.1 ± 0.2
$Ba(dpdiki)_2$ (15)	767 ± 82	706	1.1 ± 0.1
$Ba(dptriki)_2$ (16)	944 ± 76	822	1.1 ± 0.1

NMR Studies. NMR data for the free β-ketoimine ligands and corresponding Ba^{2+} complexes are compiled in the Experimental Section. All data are consistent with the proposed ligand structures and molecular connectivities. The data for the free ligands confirm the preponderance of the ketamine tautomeric form in $CDCl_3$, in accord with earlier findings for several acetylacetone-derived β-ketoimines.[18] Scalar coupling is observed between the N–H proton and the α-methylene protons of the polyether lariat, with the observed methylene multiplet collapsing to a triplet upon N–H deuteration (exposure to D_2O). ^1H and ^{13}C NMR data for 11, 12, and 13 at room temperature in C_6D_6 are consistent with a single molecular stereoisomer and/or type of ketiominate ligand. Although these results are consistent with the solid state structure of 13 (vide infra), the same result for 12, which has a less symmetrical solid-state structure (vide infra) and for 11 which is dimeric (see Table II), hence likely to have both terminal and bridging ketoiminate ligands (vide infra), implies that these complexes are stereochemically nonrigid in solution at room temperature.

In the case of complexes 14, 15, and 16, the room-temperature spectra are more complex and evidence the presence of greater than one isomer in unequal populations (only NMR data for the predominant ones are given in the Experimental Section). In the case of 15, dissolution of a single crystal in the NMR probe at −75 °C in toluene-d_8 evidences three isomers in a ~47:4:1 ratio (as judged from the well-separated methine resonances in the low-field spectral region). Warming the sample in steps to room temperature produces incremental changes in the isomer ratio, with the 30 °C populations being ~30:4:1. As for 11, 12, and 13, the simplicity of the spectra of the 14, 15, and 16 major isomers (in these cases down to −75 °C), implies intramolecular interconversion of ligand environments which is rapid on the NMR time scale. Since the solid-state structure of 14 is dimeric (vide infra), the result implies rapid interchange of bridging and terminal ketoiminate ligands. Interestingly, the isomer distribu-

(17) Purdy, A. P.; Berry, A. D.; Holm, R. T.; Fatemi, M.; Gaskill, D. K. *Inorg. Chem.* **1989**, *28*, 2799.

(18) Dudek, G. O.; Holm, R. H. *J. Am. Chem. Soc.* **1962**, *84*, 2691.

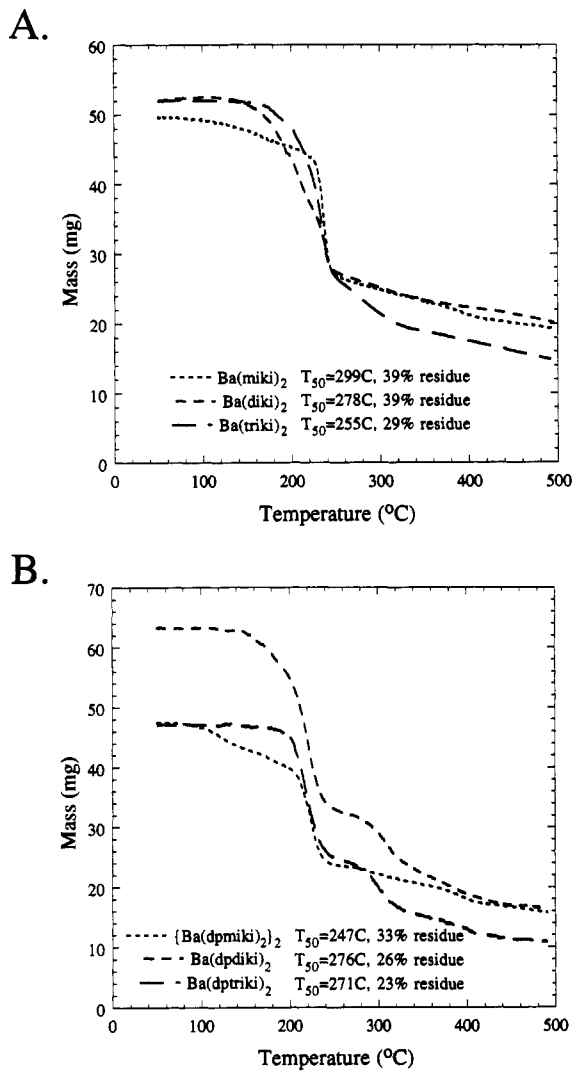

Figure 1. (A) Thermogravimetric analyses of $Ba(miki)_2$ (**11**), $Ba(diki)_2$ (**12**), and $Ba(triki)_2$ (**13**) under N_2 with a temperature ramp of 10 °C/min. (B) Thermogravimetric analyses of $\{Ba(dpmiki)_2\}_2$ (**14**), $Ba(dpdiki)_2$ (**15**), and $Ba(dptriki)_2$ (**16**) under N_2 with a temperature ramp of 10 °C/min.

tions for **14**, **15**, and **16**, are essentially identical in toluene-d_8 and THF-d_8. This suggests that THF coordination and polyether lariat displacement are not important in the latter solvent.

Thermogravimetric Analysis and Melting Points. Thermogravimetric data for **11**, **12**, **13**, and **14**, **15**, **16** which were collected under an N_2 atmosphere with a 10 °C/min temperature ramp rate, are shown in parts A and B of Figure 1, respectively. The temperature at which 50 wt % of the material has been lost is reported as T_{50} and the total weight percent residue observed at 500 °C is reported as percent residue. The T_{50}, percent residue, and melting points for all six complexes are shown in Table III. The complexes exhibit a slight decrease in percent residue as the polyether lariat is lengthened for each class of complexes (Figures 1A,B, respectively). T_{50} values show a similar behavior: decreasing T_{50} with increasing polyether lariat length with the exception of **14**. The melting points of the complexes also decrease with increasing chain length with the exception of **11**. These latter results are not surprising and are consistent with an earlier report[19] of a marked decrease in the melting points of Cu(II), Ni-

Table III. Thermogravimetric and Melting Point Data for Barium Ketoiminate Complexes

complex	T_{50} (°C)	% residue	mp (°C)
$Ba(miki)_2$ (**11**)	299	39	138–140
$Ba(diki)_2$ (**12**)	278	39	170–171
$Ba(triki)_2$ (**13**)	255	29	80–82
$\{Ba(dpmiki)_2\}_2$ (**14**)	247	33	165–168
$Ba(dpdiki)_2$ (**15**)	276	26	137–139
$Ba(dptriki)_2$ (**16**)	271	23	127–128
$Ba(dpm)_2$[a]	~360	20	
$Ba(dpm)_2$[b]	~420	25	
$Ba(dpm)_2$[c]	~360	41	

[a] Reference 6a. [b] Reference 20a. [c] Reference 20b.

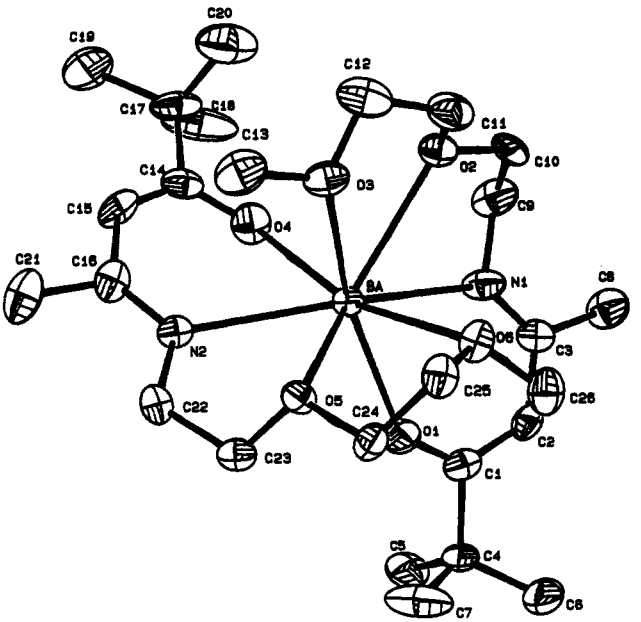

Figure 2. ORTEP drawing of the crystal structure of complex **12** showing 50% probability ellipsoids. Hydrogen atoms are omitted for clarity.

(II), and Zn(II) *N*-alkylsalicylaldiminate complexes with increased alkyl chain length. The anomalous thermal behavior of complexes **11** and **14** may be correlated with their aforementioned dimeric structures. The present barium β-ketoiminate complexes exhibit lower T_{50} temperatures than reported for various "$Ba(dpm)_2$" preparations[6a,20a,b] with roughly comparable percent residue to 500 °C values (Table III).

Single-Crystal Diffraction Studies. Crystal data and experimental details for **12**, **13**, and **14** are given in Table I with positional and equivalent isotropic thermal parameters reported for **12**, **13**, and **14** in Tables IV, V, and VI, respectively. The crystal structures of **12** and **13**, some details of which have previously been communicated,[21] are shown in Figures 2 and 3, respectively. Both complexes exhibit eight-coordinate distorted trigonal dodecahedral geometries with the terminal lariat ethoxy groups of **13** remaining uncoordinated. The metrical parameters for these two complexes (Table VII) are similar, with Ba–O(ketoiminate) distances ranging from 2.540(6) to 2.580(5) Å. The Ba–O(ether) distances in the two complexes range from 2.822(6) to 2.910(6) Å and are ~0.21–0.34 Å longer than the aforementioned Ba–O(ketoiminate) bonds. The Ba–O(ketoiminate) distances in **12** and **13** are ~0.1

(19) (a) Charles, R. G. *J. Org. Chem.* **1957**, *22*, 677. (b) Charles, R. G. *J. Inorg. Nucl. Chem.* **1959**, *9*, 145.

(20) (a) Yuhya, S.; Kikuchi, K.; Yoshida, M.; Sugawara, K.; Shiohara, Y. *Mol. Cryst. Liq. Cryst.* **1990**, *184*, 231. (b) Kim, S. H.; Cho, C. H.; No, K. S.; Chun, J. S. *J. Mater. Res.* **1991**, *6*, 704.

(21) Schulz, D. L.; Hinds, B. J.; Stern, C. L.; Marks, T. J. *Inorg. Chem.* **1993**, *32*, 249.

Table IV. Positional and Equivalent Isotropic Thermal Parameters (Å²) for 12

atom	x	y	z	B	atom	x	y	z	B
Ba	0.11815(2)	0.10614(5)	0.12982(4)	1.83(2)	C(10)	0.2098(3)	0.2860(8)	0.1541(8)	3.2(5)
O(1)	0.1446(2)	−0.0880(5)	0.1017(4)	2.9(3)	C(11)	0.1664(3)	0.3509(9)	0.2467(7)	3.6(5)
O(2)	0.1686(2)	0.2959(5)	0.1681(4)	2.6(3)	C(12)	0.1222(4)	0.379(1)	0.2452(7)	3.9(5)
O(3)	0.0991(2)	0.2794(5)	0.2417(4)	3.0(3)	C(13)	0.0560(4)	0.298(1)	0.2394(8)	4.2(6)
O(4)	0.0846(2)	0.2088(5)	−0.0083(4)	3.2(3)	C(14)	0.0514(3)	0.2702(7)	−0.0286(6)	2.6(4)
O(5)	0.0750(2)	0.066(5)	0.2484(3)	2.2(2)	C(15)	0.0142(3)	0.2478(8)	−0.0055(6)	2.8(4)
O(6)	0.1624(2)	0.0591(5)	0.3070(4)	2.9(3)	C(16)	0.0034(3)	0.1586(8)	0.0455(5)	2.6(4)
N(1)	0.1982(2)	0.1014(8)	0.0898(5)	3.0(3)	C(17)	0.0565(3)	0.3735(7)	−0.0823(6)	3.6(5)
N(2)	0.0300(2)	0.0883(6)	0.0882(4)	2.0(3)	C(18)	0.0757(6)	0.341(1)	−0.157(1)	6.6(8)
C(1)	0.1776(3)	−0.1385(7)	0.0981(5)	2.3(4)	C(19)	0.0139(4)	0.434(1)	−0.1201(9)	5.2(6)
C(2)	0.2159(3)	−0.0923(9)	0.0942(6)	2.7(4)	C(20)	0.0813(5)	0.455(1)	−0.023(1)	5.9(7)
C(3)	0.2254(3)	0.0238(8)	0.0878(6)	2.3(4)	C(21)	−0.0429(4)	0.152(1)	0.0464(7)	4.1(6)
C(4)	0.1734(3)	−0.2666(7)	0.0921(6)	2.9(4)	C(22)	0.0129(3)	0.0033(8)	0.1377(6)	2.2(4)
C(5)	0.1549(4)	−0.295(1)	−0.0031(8)	3.9(5)	C(23)	0.0465(3)	−0.0667(7)	0.1922(6)	2.3(4)
C(6)	0.2140(4)	−0.331(1)	0.120(1)	6.0(8)	C(24)	0.1020(3)	−0.0502(8)	0.3196(7)	2.5(4)
C(7)	0.1421(5)	−0.305(1)	0.143(1)	5.7(7)	C(25)	0.1348(3)	0.0294(8)	0.3628(6)	2.8(4)
C(8)	0.2692(3)	0.047(1)	0.0767(8)	3.6(5)	C(26)	0.1960(3)	−0.016(1)	0.3141(7)	3.4(5)
C(9)	0.2100(4)	0.216(1)	0.0761(9)	3.8(6)					

Table V. Positional and Equivalent Isotropic Thermal Parameters (Å²) for 13

atom	x	y	z	B	atom	x	y	z	B
Ba	0.75	0.25	0.45298(4)	1.46(2)	C(6)	0.6844(3)	−0.1621(8)	0.5898(7)	2.8(4)
O(1)	0.9061(2)	0.4405(5)	0.2423(4)	2.6(2)	C(7)	0.5914(4)	−0.144(1)	0.532(1)	4.9(5)
O(2)	0.6953(2)	0.0869(4)	0.5474(4)	2.2(2)	C(8)	0.5457(3)	0.3255(8)	0.5175(6)	2.7(4)
O(3)	0.7104(2)	0.4761(4)	0.3701(4)	1.8(2)	C(9)	0.6336(3)	0.4679(7)	0.4696(6)	2.2(4)
O(4)	0.7992(2)	0.3583(4)	0.2967(4)	2.3(2)	C(10)	0.6849(3)	0.5361(7)	0.4471(7)	2.7(3)
N	0.6438(2)	0.3353(5)	0.4938(4)	1.6(2)	C(11)	0.7555(6)	0.5471(7)	0.3332(5)	2.2(3)
C(1)	0.6463(3)	0.0570(6)	0.5574(5)	1.9(3)	C(12)	0.7809(3)	0.4738(7)	0.2567(6)	2.2(4)
C(2)	0.6035(3)	0.1373(7)	0.5421(7)	2.3(3)	C(13)	0.8352(3)	0.2879(7)	0.2383(7)	2.2(4)
C(3)	0.6016(3)	0.2698(8)	0.5164(5)	1.7(4)	C(14)	0.8928(3)	0.3130(7)	0.2650(6)	2.4(4)
C(4)	0.6348(3)	−0.0797(7)	0.5910(6)	2.4(3)	C(15)	0.9576(3)	0.4729(8)	0.2774(7)	3.5(5)
C(5)	0.6155(3)	−0.0732(8)	0.6946(8)	3.4(4)	C(16)	0.9685(4)	0.608(1)	0.257(1)	5.0(6)

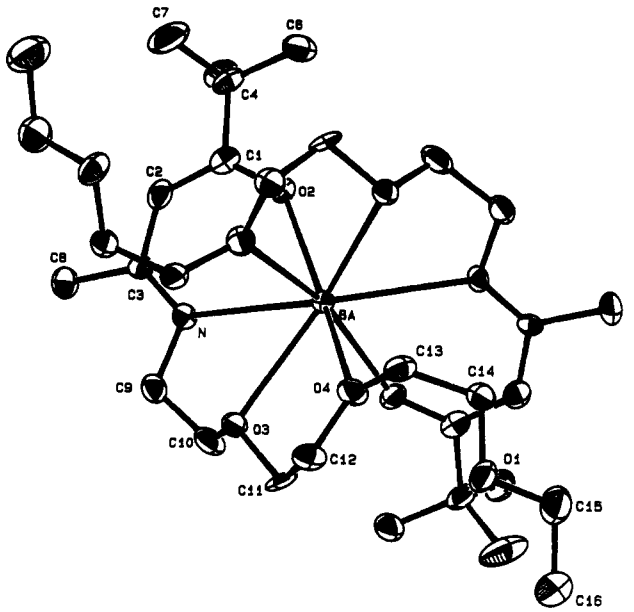

Figure 3. ORTEP drawing of the crystal structure of complex **13** showing 50% probability ellipsoids. The molecule lies on a 2-fold axis. Hydrogen atoms are omitted for clarity.

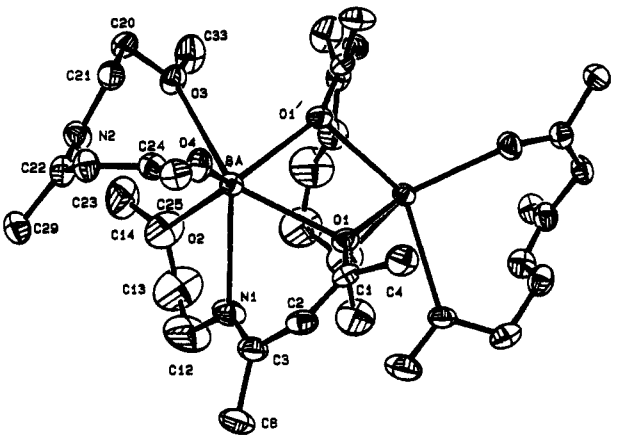

Figure 4. ORTEP drawing of complex **14** showing 50% probability ellipsoids. The molecule lies on a 2-fold axis. Hydrogen atoms and methyl groups of *tert*-butyl constituents are omitted for clarity.

Å shorter than the corresponding Ba–O(diketonate) distances in nine-coordinate Ba(β-diketonate)$_2$·tetraglyme complexes (β-diketonate = hfa, dpm, and trifluoroacetylacetonate),[5d] which range from 2.662(3) to 2.718(4) Å. This difference possibly reflects, among other factors, higher oxygen donor basicity and lower Ba^{2+} coordination numbers in the present complexes. The present Ba–O(ketoiminate) distances are appreciably longer than for typical terminal Ba–OR linkages (R = alkyl group).[22a] Ba–O(ether) distances in the aforementioned Ba(β-diketonate)$_2$·tetraglyme complexes range from 2.821(7) to 2.911(5) Å[5d] and are similar to those in **12** and **13**. Although no metrical data are available for direct comparison, Ba–N(ketoiminate) distances in **12** and **13** (2.824(7) to 2.857(5) Å) are ~0.2–0.3 Å longer than Ba–N(SiMe$_3$)$_2$ (terminal) distances in Ba[N(SiMe$_3$)$_2$]$_2$(THF)$_2$ (Ba–N = 2.587(6) and 2.596(6) Å),[22b] {Ba[N(SiMe$_3$)$_2$]$_2$(THF)}$_2$ (Ba–N = 2.602(9) Å),[22b] and {Ba[N(SiMe$_3$)$_2$]$_2$}$_2$ (Ba–N = 2.576(3) Å).[22b]

The crystal structure of **14** (Figure 4) shows that this molecule crystallizes as a dimer with two symmetry-equivalent μ_2-O(ketoiminate) atoms (O1 and O1′) bridging the two barium ions. Each Ba^{2+} exists in a six-coordinate geometry with the dimeric molecule residing on a two-fold axis. For complex **14**, two nonequivalent ketoiminate coordination modes are observed in each half of the dimer

(22) (a) Drake, S. R.; Streib, W. E.; Folting, K.; Chisholm, M. H.; Caulton, K. G. *Inorg. Chem.* **1992**, *31*, 3205 and references therein. (b) Vaartstra, B. A.; Huffman, J. C.; Streib, W. E.; Caulton, K. G. *Inorg. Chem.* **1991**, *30*, 121.

Table VI. Positional and Equivalent Isotropic Thermal Parameters (Å²) for 14

atom	x	y	z	B	atom	x	y	z	B
Ba	0.456349(8)	0.30603(2)	0.15994(1)	1.86(1)	C(10)	0.2846(2)	0.0773(7)	0.1830(3)	5.5(3)
O(1)	0.4548(1)	0.3602(3)	0.2738(1)	2.3(1)	C(11)	0.3172(2)	0.0791(8)	0.2955(3)	6.9(3)
O(2)	0.4620(2)	0.0385(3)	0.1526(2)	5.1(2)	C(12)	0.3935(3)	0.0165(6)	0.1997(3)	6.4(3)
O(3)	0.5268(1)	0.2626(3)	0.0902(1)	2.7(1)	C(13)	0.4390(3)	−0.0283(6)	0.1907(4)	7.5(4)
O(4)	0.4050(1)	0.4682(3)	0.0924(1)	2.8(1)	C(14)	0.4865(2)	−0.0307(5)	0.1158(3)	5.4(3)
N(1)	0.3943(1)	0.1523(4)	0.2115(2)	3.3(2)	C(20)	0.5181(2)	0.2981(4)	0.0278(2)	3.0(2)
N(2)	0.4307(1)	0.2512(4)	0.0083(2)	2.9(1)	C(21)	0.4676(2)	0.3533(4)	0.0110(2)	3.0(2)
C(1)	0.4112(1)	0.4092(4)	0.2690(2)	2.3(2)	C(22)	0.3846(2)	0.2804(4)	−0.0045(2)	2.6(2)
C(2)	0.3674(1)	0.3487(4)	0.2454(2)	2.7(2)	C(23)	0.3637(2)	0.4087(4)	−0.0050(2)	2.7(2)
C(3)	0.3592(2)	0.2150(5)	0.2292(2)	3.0(2)	C(24)	0.3728(1)	0.4902(4)	0.0433(2)	2.4(2)
C(4)	0.4101(2)	0.5491(4)	0.2917(2)	3.4(2)	C(25)	0.3415(2)	0.6112(4)	0.0441(2)	2.8(2)
C(5)	0.4657(6)	0.572(2)	0.3379(9)	4.8(7)	C(26)	0.3069(2)	0.5859(5)	0.0877(2)	4.2(2)
C(5B)	0.4381(7)	0.568(1)	0.3498(5)	5.1(6)	C(27)	0.3109(2)	0.6495(5)	−0.0175(2)	4.0(2)
C(6)	0.403(1)	0.643(2)	0.2469(8)	6(1)	C(28)	0.3760(2)	0.7225(4)	0.0683(2)	3.8(2)
C(6B)	0.4318(9)	0.628(1)	0.2433(8)	7.2(8)	C(29)	0.3482(2)	0.1689(4)	−0.0170(2)	3.1(2)
C(7)	0.3751(7)	0.556(1)	0.339(1)	6(1)	C(30)	0.3735(2)	0.0441(6)	−0.0208(4)	7.6(4)
C(7B)	0.3552(4)	0.605(1)	0.2814(9)	7.9(9)	C(31)	0.3199(2)	0.1620(6)	0.0332(3)	5.3(3)
C(8)	0.3089(2)	0.1577(6)	0.2373(2)	4.2(2)	C(32)	0.3112(3)	0.1913(6)	−0.0765(3)	6.6(3)
C(9)	0.2712(2)	0.2604(8)	0.2425(4)	7.4(4)	C(33)	0.5748(2)	0.2119(5)	0.1118(2)	4.1(2)

(**III**). One chelate ring is bonded in the usual O, N, O fashion with the ketoiminate oxygen and nitrogen atoms as well as the lariat ether oxygen coordinated (**III**). The

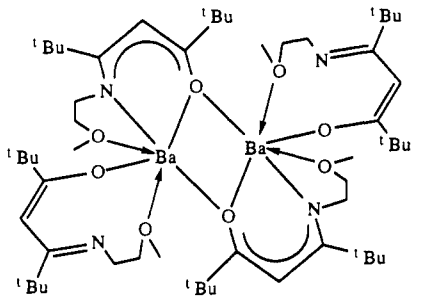

III

bridging μ_2-oxygen atom is part of this tridentate chelate ring. The other bidentate chelate ring exhibits an unusual O, O coordination mode with *both oxygen atoms* coordinated to the barium ion but not the imino nitrogen atom (Ba–N2 = 3.414(4) Å) (**III**). This unprecedented ketoiminate coordination mode may be a result of constraints imposed by the sterically demanding ^{t}Bu substituents. The two O(μ_2-ketoiminate) bridge atoms in **14** are nearly symmetrically disposed (Ba–O1 = 2.653(3) Å; Ba–O1′ = 2.665(3) Å) with bond lengths 0.06–0.22 Å shorter than Ba–O(μ_2-diketonate) distances in $[Ba(dpm)_2{\cdot}2NH_3]_2$[6b] and $[Ba(dpm)_2{\cdot}Et_2O]_2$[6d] which range from 2.77 to 2.87 Å and 2.724 to 2.826 Å, respectively. The barium ions in each of these geometrically similar dimers are bridged by four μ_2-O(diketonate) atoms which correspond to two symmetrically equivalent (both molecules possess an inversion center) β-diketonate chelates (**IV**). The difference in the

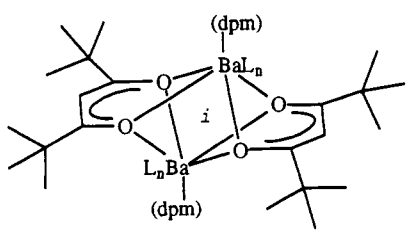

IV

extent of bridging leads to a nonbonded Ba–Ba distance in **14** (Ba–Ba = 4.297(1) Å) which is substantially longer than observed for $[Ba(dpm)_2{\cdot}2NH_3]_2$[6b] and $[Ba(dpm)_2{\cdot}Et_2O]_2$[6d] (3.83 and 3.794(1) Å, respectively). The Ba–O(ether) distances observed for **14** are similar to the corresponding distances in **12** and **13** and to the coordinated ether solvent molecules in $[Ba(dpm)_2{\cdot}Et_2O]_2$.[6d]

Table VII. Selected Bond Distances (Å) and Angles (deg) for 12, 13, and 14

12		13		14	
Ba–O1	2.575(6)	Ba–O1*	5.323(5)	Ba–O1	2.653(3)
Ba–O2	2.822(6)	Ba–O2	2.580(5)	Ba–O1′	2.665(3)
Ba–O3	2.887(6)	Ba–O3	2.841(5)	Ba–O2	2.807(3)
Ba–O4	2.540(6)	Ba–O4	2.799(5)	Ba–O3	2.790(3)
Ba–O5	2.830(5)	Ba–N	2.857(5)	Ba–O4	2.518(3)
Ba–O6	2.910(6)	O2–Ba–O2′	116.6(3)	Ba–N1	2.780(4)
Ba–N1	2.824(7)	O2–Ba–O3	126.6(1)	Ba–Ba′*	4.297(1)
Ba–N2	2.832(6)	O2–Ba–O3′	81.0(2)	Ba–N2*	3.414(4)
O1–Ba–O2	125.2(2)	O2–Ba–O4	157.6(2)	Ba–C1*	3.181(4)
O1–Ba–O3	153.0(2)	O2–Ba–O4′	85.2(2)	O1–Ba–O1′	66.6(1)
O1–Ba–O4	113.7(2)	O2–Ba–N	67.2(1)	O1–Ba–O2	106.4(1)
O1–Ba–O5	87.5(2)	O2–Ba–N′	99.9(1)	O1–Ba–O3	137.72(8)
O1–Ba–O6	82.3(2)	O2′–Ba–O3	81.0(2)	O1–Ba–O4	109.15(9)
O1–Ba–N1	65.3(2)	O2′–Ba–O3′	126.6(1)	O1–Ba–N1	65.1(1)
O1–Ba–N2	104.7(2)	O2′–Ba–O4	85.2(2)	O1′–Ba–O2	100.9(1)
O2–Ba–O3	58.0(2)	O2′–Ba–O4′	157.6(2)	O1′–Ba–O3	71.51(8)
O2–Ba–O4	85.0(2)	O2′–Ba–N	99.9(1)	O1′–Ba–O4	122.66(9)
O2–Ba–O5	123.9(2)	O2′–Ba–N′	67.2(1)	O1′–Ba–N1	117.6(1)
O2–Ba–O6	78.7(2)	O3–Ba–O3′	130.5(2)	O2–Ba–O3	75.6(1)
O2–Ba–N1	62.2(2)	O3–Ba–O4	58.3(1)	O2–Ba–O4	131.7(1)
O2–Ba–N2	129.4(2)	O3–Ba–O4′	81.7(1)	O2–Ba–N1	59.7(1)
O3–Ba–O4	93.0(2)	O3–Ba–N	60.0(1)	O3–Ba–O4	97.92(9)
O3–Ba–O5	73.1(2)	O3–Ba–N′	132.2(1)	O3–Ba–N1	135.2(1)
O3–Ba–O6	71.9(2)	O3′–Ba–O4	81.7(1)	O4–Ba–N1	108.9(1)
O3–Ba–N1	118.7(2)	O3′–Ba–O4′	58.3(1)		
O3–Ba–N2	81.7(2)	O3′–Ba–N	132.2(1)		
O4–Ba–O5	125.7(2)	O3–Ba–N′	60.0(1)		
O4–Ba–O6	162.0(2)	O4–Ba–O4′	73.5(2)		
O4–Ba–N1	94.4(2)	O4–Ba–N	116.2(1)		
O4–Ba–N2	66.6(2)	O4–Ba–N′	83.5(1)		
O5–Ba–O6	60.4(2)	O4′–Ba–N	83.5(1)		
O5–Ba–N1	138.8(2)	O4′–Ba–N′	116.2(1)		
O5–Ba–N2	59.6(2)	N–Ba–N′	156.3(20		
O6–Ba–N1	84.7(2)				
O6–Ba–N2	119.0(2)				
N1–Ba–N2	153.8(2)				

[a] Asterisks denote nonbonding interactions.

Figure 5 shows a labeled view of an ideal trigonal dodecahedron.[23] This geometry may be viewed as two interpenetrating tetrahedra. The metal coordination geometries for **12** and **13** are shown in Figure 6A,B, respectively. Figure 6A shows a distorted trigonal dodecahedral coordination for **12** with the A-type[23] atoms assignable to N1, N2, O3, and O6 and B-type[23] atoms

(23) Hoard, J. L.; Silverton, J. V. *Inorg. Chem.* **1963**, *2*, 235.

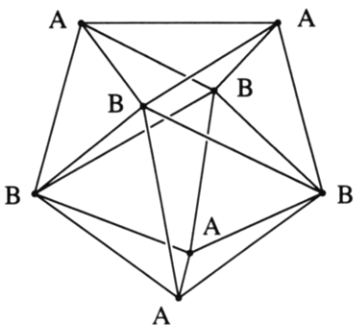

Figure 5. Geometry of a perfect trigonal dedecahedron showing the atom labeling scheme.

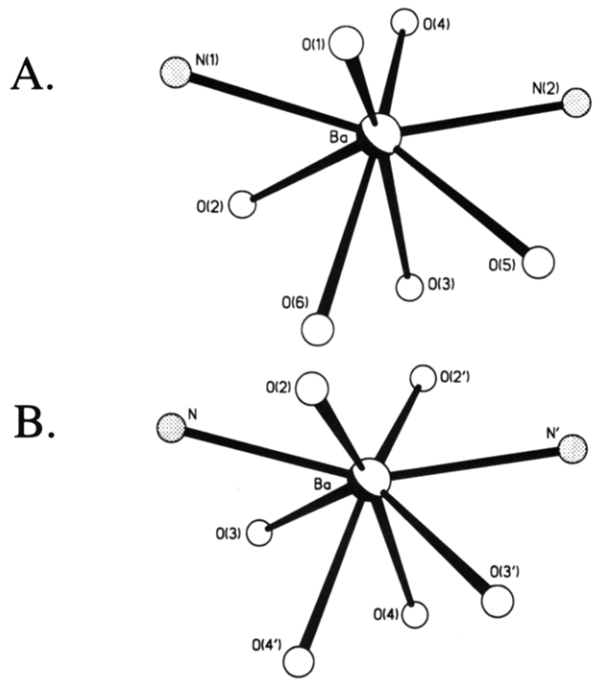

Figure 6. (A) Immediate Ba^{2+} coordination geometry of complex **12**. (B) Immediate Ba^{2+} coordination geometry of complex **13**.

assignable to O1, O4, O2, and O5. Figure 6B shows a distorted trigonal dodecahedral coordination for **13** with the A-type atoms assignable to N, N′, O4, and O4′ and B-type atoms assignable to O2, O2′, O3, and O3′. For both complexes **12** and **13**, the ketoiminate oxygens and the first lariat ether oxygens can be assigned to B-type atoms while the ketoiminate nitrogens and the second lariat ether oxygens can be assigned to A-type atoms. Each structure exhibits a distortion of the A-type atoms with the N–Ba–N angle being larger (153.8(2) and 156.3(2)° for **12** and **13**, respectively) and the O–Ba–O angle smaller (71.9(2) and 73.5(2)° for **12** and **13**, respectively) than the expected 109°. This distortion from ideal dodecahedral coordination is due to the geometric constraints imposed by the unsymmetrical β-ketoiminate ligation.

A distorted trigonal dodecahedral coordination polyhedron is assigned for both eight-coordinate complexes, **12** and **13**, after analyzing their structures versus the other likely eight-coordinate polyhedron, the square antiprism. A semiquantitative analysis[24] considers a dodecahedron or square antiprism to consist of two mutually perpendicular trapezoids. Each of the two trapezoid planes are defined by the metal center, two A-type atoms, and two B-type atoms; the intersecting angle of which provides a measure to distinguish between dodecahedral and square

(24) Lippard, S. J.; Russ, B. J. *Inorg. Chem.* **1968**, *7*, 1686.

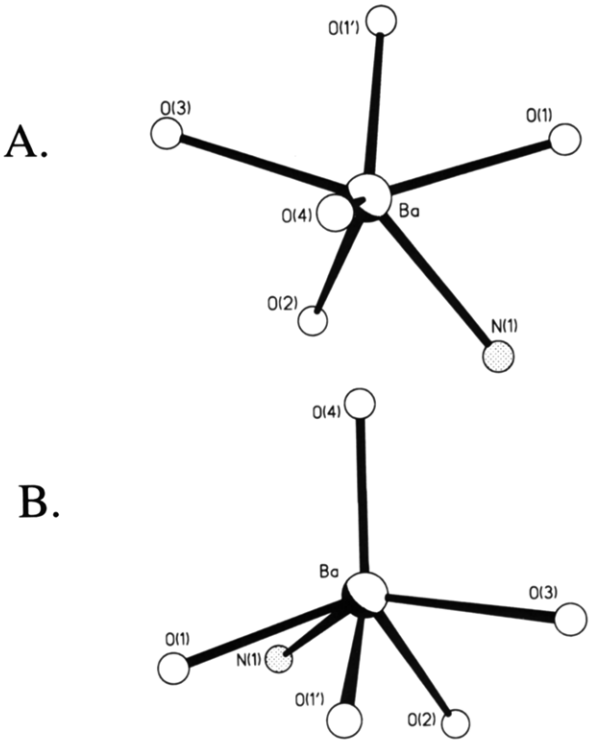

Figure 7. (A) Immediate Ba^{2+} coordination geometry of complex **14** viewed perpendicular to the least-squares pentagonal plane. (B) Immediate Ba^{2+} coordination geometry of complex **14** viewed parallel to the least-squares pentagonal plane.

antiprismatic coordination geometries. For example, the angle between the two intersecting trapezoid planes which define a perfect dodecahedron is 90.0° versus 77.4° for a perfect square antiprism. Upon careful examination of the possible planes for complex **12**, the following atoms were determined to define the best fit (mean deviation from planarity) least-squares trapezoid planes 1 and 2, respectively: Ba, O1, O4, O3, and O6; Ba, O2, O5, N1, and N2. The equations which define planes 1 and 2 for complex **12** are given in orthogonal coordinates as eqs 2 and 3 with

$$0.8517X + 0.4362Y - 0.2903Z = 3.4599 \quad (2)$$

$$0.3154X + 0.0636Y + 0.9468Z = 2.6677 \quad (3)$$

mean deviations of 0.147 and 0.784 Å, respectively. The angle between these two planes was calculated to be 88.8°. Upon careful examination of the possible planes for complex **13**, the following atoms were determined to define the best fit (mean deviation from planarity) least-squares trapezoid planes 1 and 2, respectively: Ba, O2, O2′, O4, and O4′; Ba, N, N′, O3, and O3′. The equations which define planes 1 and 2 for complex **13** are given in orthogonal coordinates as eqs 4 and 5 with mean deviations of 0.112

$$0.7479X - 0.6638Y + 0.0000Z = 12.2390 \quad (4)$$

$$0.0000X + 0.0000Y + 1.0000Z = 6.2585 \quad (5)$$

and 0.758 Å, respectively. The angle between these two planes was calculated to be 90.0°. Intersecting angles of 88.8° and 90.0° for the trapezoid planes which define **12** and **13**, respectively, substantiate a distorted dodecahedral coordination assignment for each complex versus distorted square antiprismatic.

Figure 7 shows that the local coordination geometry about each barium ion of the symmetrical dimer **14** is distorted pentagonal pyramidal. A least-squares plane

calculated using the atoms which define the pentagonal base (i.e., O1, O1′, O2, O3, and N1) is given by eq 6

$$0.6072X - 0.6220Y + 0.4944Z = 7.1120 \quad (6)$$

for orthogonal coordinates. The mean deviation from planarity for these five atoms is 0.465 Å with Ba lying −1.086 Å and O4 residing −3.598 Å from the least-squares plane. The view in Figure 7A is drawn perpendicular to the least-squares plane showing the nearly 5-fold axis. Figure 7B is drawn parallel to the least-squares plane and shows the apical O4 atom. This unusual coordination geometry does not take into account relatively close barium contacts with N2 and C1—3.414(4) and 3.181(4) Å, respectively.

Vapor Transport Properties and Thermolysis Mechanism. All six barium β-ketoiminate complexes can be sublimed under reduced pressure (10^{-3} Torr) at temperatures between 150 and 200 °C. Since several of the complexes melt near the temperature required for efficient transport, in some cases the term sublimation is in fact liquid vaporization. Although these complexes exhibit appreciable volatility, sublimation is invariably accompanied by some degree of thermal decomposition. The major volatile thermolysis product is invariably the free ligand (HL). In some instances, free ligand droplets collect at the top of the coldfinger, with the less volatile barium complex condensing on the bottom. In other cases, the ligand and complex condense together at the bottom of the coldfinger. Resublimation of the sublimed complex results in a similar decomposition pattern. The temperature dependence of the ratio of transported BaL_2:HL was briefly investigated, and it was found that higher temperatures result in a larger transport ratio, i.e., higher yields of transported barium ketoiminate complexes. In the case of **12** at or below a sublimation temperature of 100 °C/7 × 10^{-3} Torr, only HL collects on the water-cooled coldfinger, even after 26 h. When the remaining solid is then brought to 150 °C/7 × 10^{-3} Torr for 48 h, a mixture of BaL_2 and HL is collected, with 15% by weight of the original sample mass remaining as a nonvolatile orange residue. The overall mass balance for this experiment is a ~1:4 molar ratio of BaL_2:HL transferred to the coldfinger. In another experiment, the **12** was transported at 200 °C (above the melting point)/7 × 10^{-3} Torr for 2 h at which time only 14% of the original mass remained as an orange residue. In this instance, ^{1}H NMR integration and mass balance determination gives a BaL_2:HL molar ratio ~5:1. These results appear to reflect differing activation enthalpies for thermolysis versus sublimation, as well as differences in ketoiminate volatility above the melting point.

Elemental analysis of the orange residue which remained after sublimation of **11** at 200 °C/7 × 10^{-3} Torr for 2 h gave C:H:N:Ba weight percent ratio of 33.19% C, 4.84% H, 1.62% N, and 41.07% Ba. Assuming oxygen comprises the remaining 19.28% of the sample, this corresponds to an empirical formula for the residue of $Ba_1C_{9.2}H_{16.1}N_{0.4}O_{4.0}$. By comparison of the molar content of barium in the residue versus in the starting sample, it was determined that the sublimation at 200 °C/7 × 10^{-3} Torr for 2 h transported 84% of the barium.

Experiments aimed at characterizing the mechanism of the formation of HL from BaL_2 were performed according to the following procedure. A standard sublimer equipped with a water-cooled cold finger was loaded in the glovebox with a weighted sample of **11**, **12**, or **13** contained in a platinum boat. Next, ~2 mL of C_6D_6 was added to a 100-mL Schlenk flask. The Schlenk flask was then attached to the vacuum port of the sublimer with high vacuum hose, and the apparatus was removed from the glovebox. Next, as the entire apparatus was brought under dynamic vacuum ((6–9) × 10^{-3} Torr), the Schlenk flask was cooled to 77 K, the coldfinger was cooled with water, and the sublimer bottom immersed in a 200 °C oil bath. In every experiment, a yellow liquid formed in the platinum boat at the onset since the melting points for complexes **11**, **12**, and **13** are all below 200 °C. Each experiment provided four major products which were characterized by ^{1}H NMR, GC/MS, and/or MS: an orange residue in the platinum boat, a mixture of HL and BaL_2 on the coldfinger, and volatile thermolysis products which collected in the 77 K trap.

The orange thermolysis residues of **11**, **12**, and **13** are initially soluble in CD_3OD. However, solids which are presumably polymeric barium alkoxides, precipitate over the course of several days under an N_2 atmosphere. ^{1}H NMR spectra of freshly prepared solutions of these residues in CD_3OD exhibit several interesting features. First, no methine resonances are observed, indicating that the ketoiminate ligands do not remain intact during the thermolysis. Control studies of Hmiki in CD_3OD rule out the possibility that the methine proton undergoes signficant deuterium exchange. Second, the region δ 3.3–3.9 exhibits resonances which correspond to the polyether lariat substituents of the parent ketoiminate chelates. However, for each thermolysis residue, one less set of CH_2-CH_2 resonances is observed versus the starting complex. For example, the ^{1}H NMR spectrum of the thermolysis residue of **11** shows only one singlet in the δ 3.3–3.0 region versus one singlet and two triplets in the same region for pure **11**. Likewise, the ^{1}H NMR spectrum of the thermolysis residue of **12** shows one singlet and only two triplets at δ 3.3–3.9 versus one singlet and four triplets in the same region for pure **12**. The ^{1}H NMR spectrum of the thermolysis residue of **13** exhibits a similar pattern with a triplet resonance at δ ~1.10, indicating the terminus of this lariat remains intact. The identified physical observable and major component in each ^{1}H NMR spectrum is an ROD fragment. The OR groups in each of the fragments correspond to a lariat polyether less one ethylene linkage. MS of the residues subsequent to dissolution in CD_3OD and evaporation shows ions corresponding to ROD. These observations suggest that "lariat cleavage" likely occurs at the C–O bond β to the ketoiminate nitrogen (e.g., eq 7). The structure(s) of other **11**, **12**, **13** thermolysis

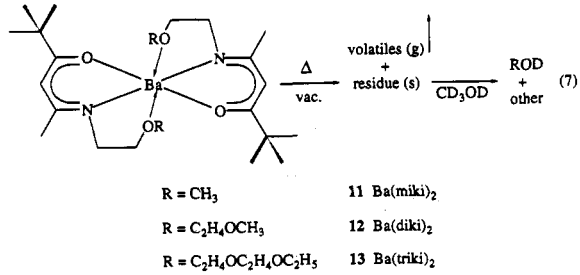

R = CH_3 **11** Ba(miki)$_2$

R = $C_2H_4OCH_3$ **12** Ba(diki)$_2$

R = $C_2H_4OC_2H_4OC_2H_5$ **13** Ba(triki)$_2$

residue components could not be unambiguously assigned from MS and ^{1}H NMR data, however, the following singlet ^{1}H NMR features are invariably observed in CD_3OD with the relative intensities indicated: δ 1.10 (s, 5H), 1.89 (s, 1H), 1.94 (s, 1H), 2.02 (s, 1H).

MS of the thermolysis residues before dissolution exhibit OR fragments which may arise from a barium alkoxide, such as XBaOR. No barium-containing ions were noted

Scheme II. Possible Thermal Decomposition Pathway for BaL_2 Complexes

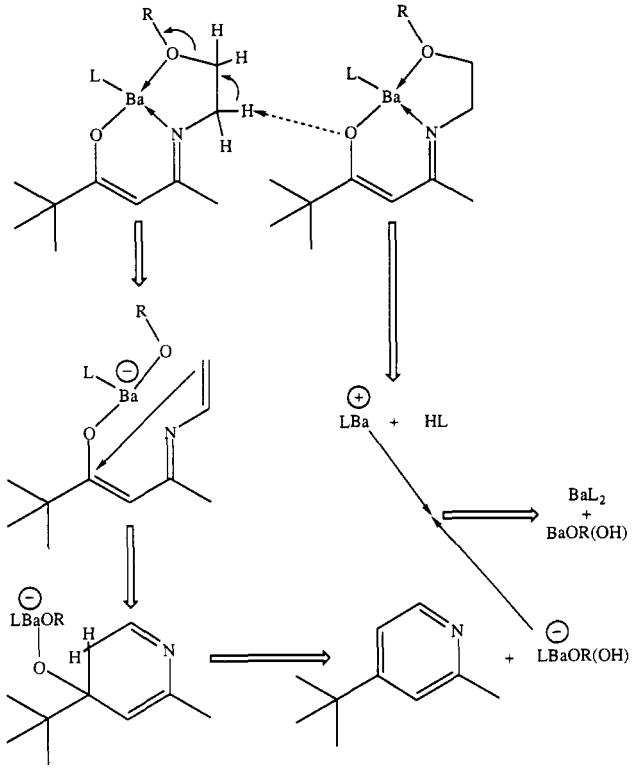

in these MS data. Simple XBaOR species such as $Ba(OCH_3)_2$, $Ba(OCH_3)L$ (L = miki), and $Ba(OCH_3)(OH)$ have calculated elemental formulas ($Ba_1C_2H_6N_0O_2$, $Ba_1C_{12}H_{22}N_1O_3$, and $Ba_1C_1H_4N_0O_2$, respectively) which are not consistent with the observed elemental analysis of the 11 thermolysis residue $Ba_1C_{9.2}H_{16.1}N_{0.4}O_{4.0}$. The actual composition of the residue may be oligomeric and/or a mixture of these and/or other species; the sum of which explain the observed elemental analysis.

^1H NMR and GC/MS analysis of the thermolysis components collected in the 77 K trap shows the presence of pinacolone, 2,2-dimethyl-5-imino-3-hexanone, and a new compound, 2-methyl-4-*tert*-butylpyridine (17) which was

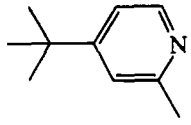

17

characterized by ^1H NMR and high-resolution GC/MS.[25] The observation of 17 coupled with the aforementioned "lariat cleavage" provides the basis for a possible ketoiminate thermolysis pathway (Scheme II). The first step is base-catalyzed elimination between two neighboring BaL_2 complexes to form a vinylimine barium anion, a barium cation (BaL^+), and free ligand (HL). Disrotatory electrocyclic ring closure of the aforementioned anionic intermediate followed by 1,2 elimination of $BaLOR(OH)^-$ yields 17. Finally, an acid–base reaction between the cation and anion gives $BaOR(OH)$ and BaL_2. The proposed pathway provides an explanation for most of the major thermolytic observables: free ligand on the coldfinger, lariat alkoxide less one ethylene group in the residue, and 17 in the 77 K trap. The proposed pathway is unusual in that most pyridine syntheses from acyclic compounds require the formation of a carbon–nitrogen bond.[26] Furthermore, there is precedent for this type of ring closure.[27]

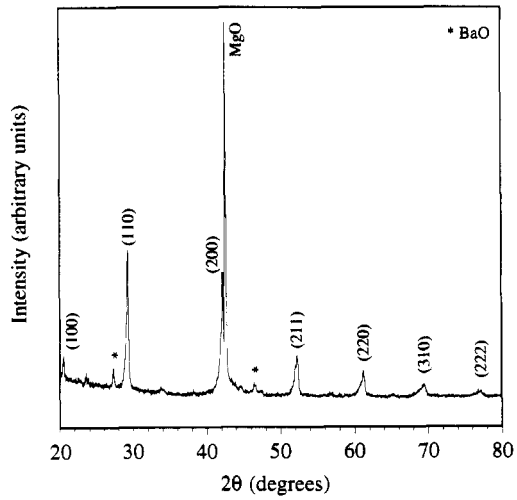

Figure 8. θ–2θ X-ray diffraction scan for a $BaPbO_3$ thin film grown by MOCVD using 12 and $Pb(dpm)_2$ after a postdeposition anneal for 5 min at 890 °C in air.

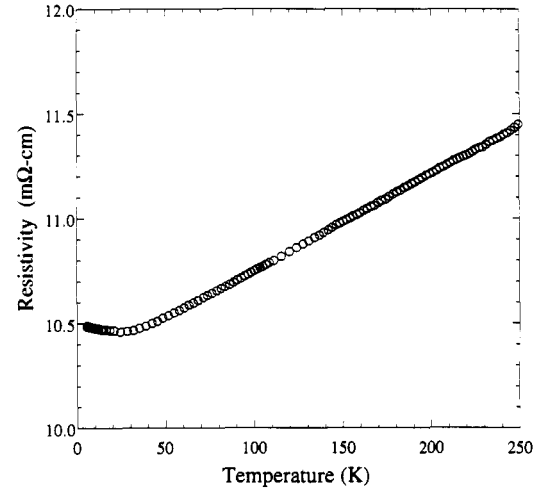

Figure 9. Variable-temperature four-probe resistivity data for the MOCVD-derived $BaPbO_3$ film shown in Figure 8.

MOCVD of $BaPbO_3$ Films Using β-Ketoiminate Precursors. Thin films of the metallike perovskite phase $BaPbO_3$[10] were grown by MOCVD to demonstrate the efficacy of "lariat" ketoiminate complexes as barium MOCVD precursors. Experiments were carried out with 12 and $Pb(dpm)_2$ (see Experimental Section for details). The as-deposited films were amorphous by X-ray diffraction with the $BaPbO_3$ phase forming during a 5-min postanneal at 890 °C in air. A θ–2θ X-ray diffraction scan of a 1.4-μm-thick film (Figure 8) shows it to consist of crystalline $BaPbO_3$[28] with traces of contaminating BaO.[28] The presence of trace BaO is consistent with SEM/EDX data which give a Ba:Pb ratio slightly greater than 1.0. A

(25) 2-Methyl-4-*tert*-butylpyridine (17): ^1H NMR (300 MHz, C_6D_6) δ 1.30 (s, 9H), 2.59 (s, 3H), 6.72 (m, 1H, J_{ab} = 5.2 Hz), 6.91 (s, 1H), 8.49 (m, 1H, J_{ab} = 5.2 Hz). MS (EI, 70 eV, *m/e*+; (fragment); M = 17) 149 (M), 134 (M – CH_3), 92 (M – $C(CH_3)_3$). Calcd for $C_{10}H_{15}N$ (M) 149.1204; found 149.1206. Calcd for $C_9H_{12}N$ (M – CH_3) 134.0969; found 134.0972.

(26) Boodman, N. S.; Hawthorne, J. O.; Masciantonio, P. X.; Simon, A. W. In *Pyridine and Its Derivatives*; Abramovitch, R. A., Ed.; John Wiley & Sons: New York, 1974; pp 183–307.

(27) Jones, R. G. *J. Am. Chem. Soc.* **1951**, *73*, 5244.

(28) Joint Committee on Powder Diffraction Standards (JCPDS), center for Diffraction Data, 1601 Park Lane, Swarthmore, PA; No. 12-664 ($BaPbO_3$); No. 1-746 (BaO).

variable-temperature resistivity plot of an MOCVD-derived $BaPbO_3$ film is shown in Figure 9. The resistivity of the sample decreases modestly upon cooling, in excellent agreement with previously noted metallike transport properties.[10]

Conclusions

A new class of volatile barium coordination complexes based upon multidentate ketoiminate ligation has been successfully synthesized and characterized. The utility of these complexes as precursors to barium oxide-containing thin films by MOCVD has been demonstrated through the growth of $BaPbO_3$ films. These complexes have well-defined, reproducible stoichiometries with thermal characteristics similar or superior to the commonly used barium MOCVD precursor, "$Ba(dpm)_2$". All of these barium ketoiminate complexes partially decompose during sublimation. A plausible decomposition pathway has been proposed which involves ligand fragmentation at the C–O bond β to the ketoiminate nitrogen atom.

Acknowledgment. This work was funded by the National Science Foundation through the Science and Technology Center for Superconductivity (NSF Grant DMF 9120000) and the Northwestern University Materials Research Center (NSF Grant DMR 8821571). The authors thank Dr. Doris Hung for mass spectrometric analyses, Mr. Jon L. Schindler and Prof. Carl R. Kannewurf for the variable-temperature resistivity characterization, Prof. R. P. H. Chang for access to the profilometer, and Mr. Michael Giardello and Dr. Paul Deck for assistance with NMR experiments and helpful discussions.

Supplementary Material Available: Crystal structure analysis report including tables of hydrogen atom coordinates, anisotropic thermal parameter, bond lengths, bond angles, crystallographic data, and completely labeled ORTEP plots for **12**, **13**, and **14** (33 pages); tables of crystal structure factors for **12**, **13**, and **14** (33 pages). Ordering information is given on any current masthead page.